© 2017. Published by The Company of Biologists Ltd | Development (2017) 144, 3744-3754 doi:10.1242/dev.148684

RESEARCH ARTICLE

A radial axis defined by semaphorin-to-neuropilin signaling controls pancreatic islet morphogenesis

Philip T. Pauerstein[1], Krissie Tellez[1], Kirk B. Willmarth[1], Keon Min Park[1], Brian Hsueh[2], H. Efsun Arda[1], Xueying Gu[1], Haig Aghajanian[3], Karl Deisseroth[2,4], Jonathan A. Epstein[3] and Seung K. Kim[1,*]

ABSTRACT

The islets of Langerhans are endocrine organs characteristically dispersed throughout the pancreas. During development, endocrine progenitors delaminate, migrate radially and cluster to form islets. Despite the distinctive distribution of islets, spatially localized signals that control islet morphogenesis have not been discovered. Here, we identify a radial signaling axis that instructs developing islet cells to disperse throughout the pancreas. A screen of pancreatic extracellular signals identified factors that stimulated islet cell development. These included semaphorin 3a, a guidance cue in neural development without known functions in the pancreas. In the fetal pancreas, peripheral mesenchymal cells expressed Sema3a, while central nascent islet cells produced the semaphorin receptor neuropilin 2 (Nrp2). Nrp2 mutant islet cells developed in proper numbers, but had defects in migration and were unresponsive to purified Sema3a. Mutant Nrp2 islets aggregated centrally and failed to disperse radially. Thus, Sema3a-Nrp2 signaling along an unrecognized pancreatic developmental axis constitutes a chemoattractant system essential for generating the hallmark morphogenetic properties of pancreatic islets. Unexpectedly, Sema3a- and Nrp2-mediated control of islet morphogenesis is strikingly homologous to mechanisms that regulate radial neuronal migration and cortical lamination in the developing mammalian brain.

KEY WORDS: Islet, Chemoattractant, Radial migration, Nrp2, Sema3a, Neural development, Cortex, Mouse, Human

INTRODUCTION

Pancreatic islets are named for their most characteristic feature: islets are endocrine cell clusters dispersed throughout an abundant sea of exocrine tissue. The molecular and signaling origins of this conserved hallmark morphology, which are established during fetal development, remain undefined. Islets are endocrine micro-organs that are crucial for regulation of metabolism, including glucose control. Within the islets, β cells secrete insulin to stimulate glucose uptake by peripheral tissues and α cells secrete glucagon to mobilize glucose from target organs such as the liver. Islet structure may influence function: specialized vascular and neural crest-derived structures ramify within islets to regulate hormone secretion and blood flow, and interactions among islet cells can influence hormone secretion (Brissova et al., 2006; Cleaver and Dor, 2012; Lammert et al., 2003; Muñoz-Bravo et al., 2013; Reinert et al., 2014; Rodriguez-Diaz et al., 2011; van der Meulen et al., 2015). Islet morphogenesis comprises several distinct processes. Initially, islet formation begins with delamination of endocrine precursor cells from the primitive core of the branching ductal epithelium. After exiting this epithelial layer, newborn islet cells migrate away from the epithelium into the surrounding mesenchyme, cluster and begin to form recognizable islets (Benitez et al., 2012; Gouzi et al., 2011; Rukstalis and Habener, 2007). Vascularization and innervation of islets begins in the embryo and continues postnatally (Reinert et al., 2014), and islets appear to continue to disperse from large central ductal structures after birth, although this latter process has not been measured. Thus, islet morphogenesis could be parsed into delamination, migration, clustering and remodeling, with the possibility that each of these processes could be controlled by distinct signals. Despite the importance of islet structure to function, little is known regarding long- or short-range signals that control islet morphogenesis.

Prior studies have identified secreted signals controlling cell differentiation and proliferation in pancreas development (reviewed by Benitez et al., 2012; Gittes, 2009; Kim and Hebrok, 2001; Puri and Hebrok, 2010; Serup, 2012). For example, classical fetal organ culture studies showed that pancreatic mesenchyme provides cues for epithelial expansion, morphogenesis and differentiation (Gittes et al., 1996; Golosow and Grobstein, 1962; Landsman et al., 2011; Wessells and Cohen, 1967). Studies by Bhushan et al. (2001) revealed that Fgf10, which is expressed throughout the pancreatic mesenchyme at the inception of pancreas morphogenesis, is required for pancreatic progenitor proliferation. Other studies demonstrated that vascular endothelium induces foregut expression of *Ptf1a* and *Pdx1*, crucial transcriptional regulators of pancreatic growth and development (Lammert et al., 2001; Yoshitomi and Zaret, 2004). At later stages, Notch signaling – possibly through short-range lateral inhibition – controls endocrine cell specification and acinar cell differentiation from progenitor cells (Afelik et al., 2012; Apelqvist et al., 1999; Cras-Méneur et al., 2009; Esni et al., 2004; Murtaugh et al., 2003; Shih et al., 2012). Short-range signals associated with neural development, including netrins and Eph-ephrin signaling, have been associated with pancreatic cell migration, growth and islet function (Konstantinova et al., 2007; Yang et al., 2011; Yebra et al., 2003). In islet morphogenesis, extracellular signals, including EGF, HGF and TGFβ, and intracellular signal transducers, including Cdc42, Rac1, Tm4sf4 and Grg3 have been suggested to influence fetal islet morphogenesis (Anderson et al., 2011; Blum et al., 2014; Greiner et al., 2009; Guo et al., 2013; Kesavan et al., 2014; Metzger et al., 2012; Miettinen et al., 2000; Miralles et al., 1998; Pagliuca et al.,

[1]Department of Developmental Biology, Stanford University School of Medicine, Stanford, CA 94305, USA. [2]Departments of Bioengineering and of Psychiatry and Behavioral Sciences, Stanford University School of Medicine, Stanford, CA 94305, USA. [3]Department of Cell and Developmental Biology, Perelman School of Medicine at the University of Pennsylvania, Philadelphia, PA 19104, USA. [4]Howard Hughes Medical Institute, Stanford University School of Medicine, Stanford, CA 94305, USA.

*Author for correspondence (seungkim@stanford.edu)

K.B.W., 0000-0002-8378-1732; S.K.K., 0000-0001-6135-7810

Received 4 January 2017; Accepted 4 September 2017

Development (2017) 144, 3744-3754 doi:10.1242/dev.148684

2014; Rezania et al., 2014; Sanvito et al., 1994; Tulachan et al., 2007). Thus, although many signals are known to regulate pancreas and islet development, spatially localized cues that might control islet morphogenesis have not yet been discovered.

To define signals controlling islet cell migration and movement, we designed a screen to identify secreted factors sufficient to alter β cell localization in development. We characterized one factor identified in the screen, semaphorin 3a, as a regulator of fetal islet cell migration during islet morphogenesis. The Sema3 family is composed of secreted proteins initially identified as inducers of axon growth cone collapse, and later characterized as chemoattractant or chemorepulsive factors that regulate multiple specific stages of nervous system development, including axon targeting, neuron migration and neuron polarization (Chen et al., 2008; Kolodkin et al., 1993; Polleux et al., 1998; Shelly et al., 2011; Tran et al., 2009). In addition, semaphorins have been demonstrated to function in other organ systems, including bone homeostasis and cardiovascular development (Degenhardt et al., 2013; Epstein et al., 2015; Fukuda et al., 2013; Ieda et al., 2007). Secreted semaphorins usually signal through heterodimeric receptor complexes composed of neuropilins and plexins (Chen et al., 1997; Giger et al., 2000; Kolodkin et al., 1997; Takahashi et al., 1999; Tamagnone et al., 1999; Winberg et al., 1998). Neuropilin 2 (Nrp2) expression has been reported in adult islets and *Sema3a* mRNA was enriched in E11.5 mouse pancreatic mesenchyme (Cohen et al., 2002; Guo et al., 2013), but a functional role for semaphorin signaling has not yet been reported in pancreatic development or physiology.

Here, we provide evidence that semaphorin signaling through Nrp2 receptors during pancreas development provides guidance cues along a previously unrecognized proximodistal axis that is essential for regulating islet morphogenesis and dispersion. This developmental signaling axis in the pancreas has striking homology to radial patterning cues required for cortical lamination during neural development, unexpectedly revealing shared use of a signaling module to establish radial pattern in the brain and pancreas.

RESULTS

A screen to identify morphogenetic signals controlling islet development

To define signals controlling islet cell migration, we identified 21 candidate secreted factors based on existing genome-wide expression datasets from fetal pancreatic mesenchyme (Guo et al., 2013) and developing islet cells (Benitez et al., 2014). To assay for effects on islet development, we implanted factor-soaked beads in cultured E13.5 *Ins1*-GFP transgenic mouse fetal pancreas (Fig. 1A, Fig. S1) (Hara et al., 2003). By measuring changes in the

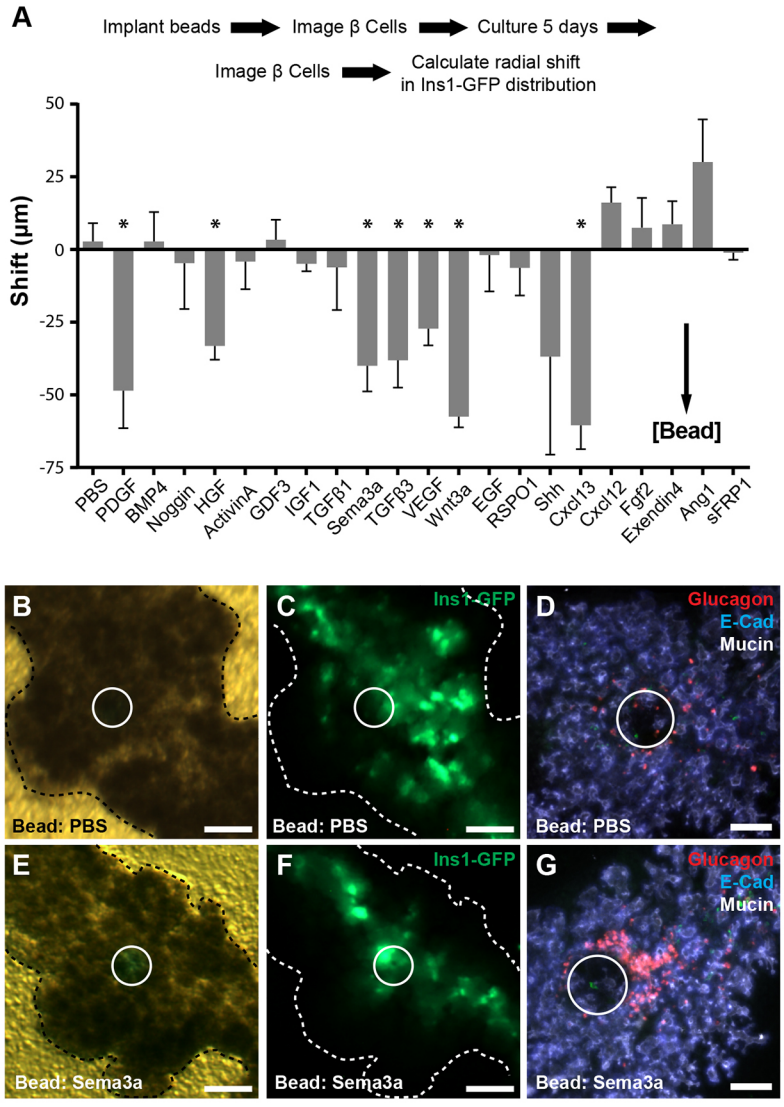

Fig. 1. Development of a screen to identify secreted signals regulating islet development. (A) Schematic of bead screen workflow (see Fig. S1 for details). Results of a screen of 21 candidate signals. Statistical significance is indicated (*P<0.05, two-tailed t-test; see Table S1 for n for each signal). (B-D) *Ins1*-GFP fluorescence is distributed throughout the organ with PBS beads, and α cells were distributed randomly around beads, as detected by whole-mount immunofluorescence. (E,F) *Ins1*-GFP signal is redistributed toward the epithelial core with Sema3a-soaked beads. (G) In the distal dorsal pancreas, α cells cluster around Sema3a-soaked beads. White circles indicate bead location. Scale bars: 100 μm. Data are mean±s.e.m.

Development (2017) 144, 3744-3754 doi:10.1242/dev.148684

distribution of β cell-derived GFP signal around beads over 5 days of development, we identified seven growth factors that increased β cell proximity to beads (Fig. 1A). These included growth factors with established roles in islet biology, including PDGF, VEGF and HGF (Cai et al., 2012; Chen et al., 2011; Reinert et al., 2013, 2014; Roccisana et al., 2005), and ligands with unknown function in islet development, including Cxcl13 and Sema3a. Based on this β cell clustering and the pronounced α cell phenotypes described below, we chose semaphorin signaling for further study.

Pancreatic β cell distribution was strongly shifted toward beads soaked in Sema3a (P=0.01 relative to PBS control beads, Fig. 1B,C,E,F). We also observed clustering of glucagon$^+$ α cells adjacent to Sema3a-soaked beads by immunofluorescence analysis (Fig. 1D,G). Quantification of α cell fluorescence relative to beads demonstrated that glucagon$^+$ cells were significantly increased near Sema3a-soaked beads compared with PBS-soaked control beads (P=0.04, two tailed t-test: Sema3a=2348±254 versus PBS=1506±61). Many α cells lacked E-cadherin expression, consistent with acquisition of a migratory phenotype (Acloque et al., 2009). Moreover, unlike α cells in PBS controls, α cells adjacent to Sema3a-soaked beads were deep in the mesenchyme several cell diameters from nearby ductal epithelia, suggesting that Sema3a might affect islet cell migration over a relatively long range (Fig. S1). Expression of Ki67 in glucagon$^+$ cells remained unchanged by Sema3a-soaked beads at multiple time points tested, suggesting that increased α cell proliferation did not underlie the observed phenotypes (Fig. S1). Likewise, expression of the islet progenitor marker Neurog3 was indistinguishable in organs implanted with PBS or Sema3a-soaked beads, indicating that Sema3a did not induce endocrine differentiation (Fig. S1). Other semaphorin family members, including *Sema3b* and *Sema3f*, were expressed in the pancreas at E15.5, and in bead experiments had similar effects on fetal α cell localization (Fig. S1). These data suggested that semaphorin signaling might provide guidance cues to migrating fetal islet cells.

Radial asymmetry in distribution of semaphorin signaling components in the developing pancreas

Based on established roles of semaphorins as chemoattractant or chemorepulsant guidance cues in other contexts, we next assessed whether semaphorin signaling might provide directional cues in islet morphogenesis. At E15.5, *in situ* hybridization revealed a striking concentration of *Sema3a* transcripts at the pancreatic mesenchymal periphery. By contrast, we observed uniform distribution of *Polr2a* transcripts encoding RNA polymerase II (Fig. 2A-C). Developing islet cells, including glucagon$^+$ α cells, were localized to the core of the organ, adjacent to the central epithelium (Fig. 2A-C). Cells expressing *Sema3a* co-expressed the fibroblast marker vimentin and were enriched in FACS-purified mesenchymal cells in the fetal pancreas, supporting the view that peripheral fibroblasts expressed *Sema3a* (Fig. S2). We observed a similar peripheral mesenchymal localization of *Sema3d* using Sema3d$^{GFP/Cre}$ knock-in mice (Katz et al., 2012) and by measuring gene expression in FACS-purified cell populations (Fig. S2). Compared with Sema3a expression, Sema3d^{gfp} expression appeared to extend several cell layers deeper, suggesting that a semaphorin gradient composed of multiple types of semaphorins could instruct islet morphogenesis. Alternatively, this difference in observed expression pattern could reflect differences in detecting Sema3a by *in situ* hybridization and Sema3d by GFP expression.

In contrast to Sema3 ligand production in peripheral mesenchyme, we detected the Sema3 receptor Nrp2 in both α and β cells at E13.5

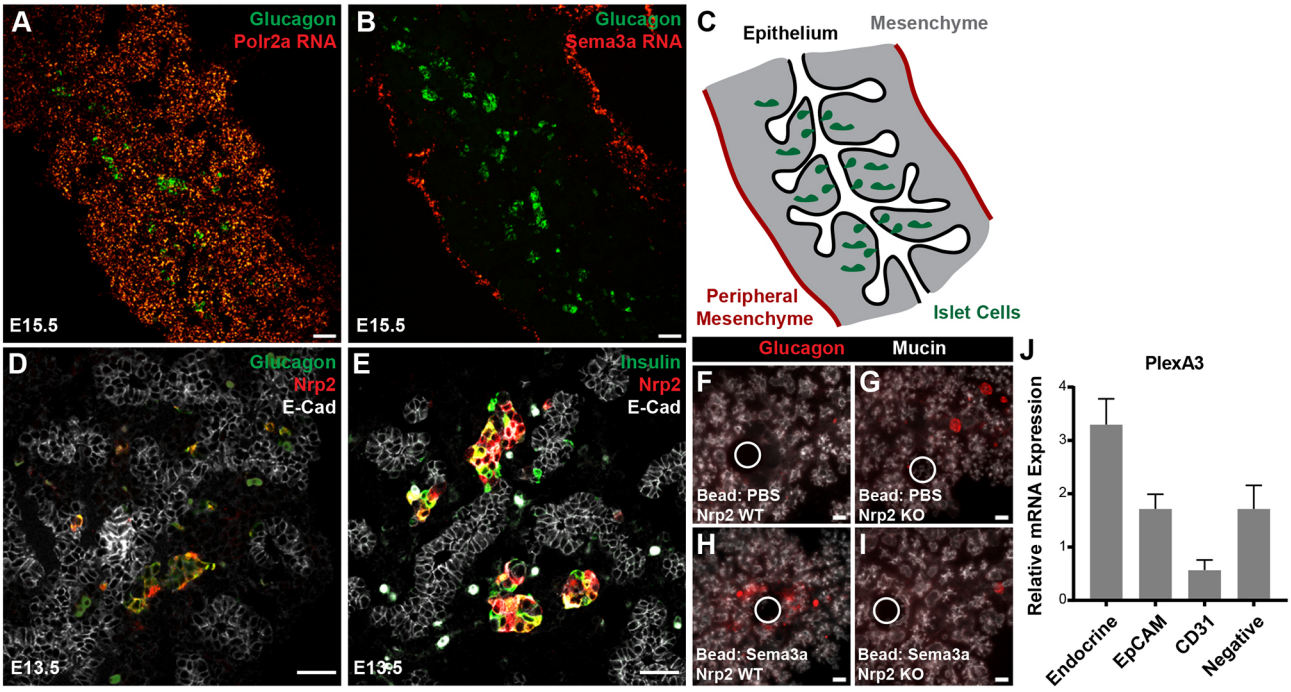

Fig. 2. Radial asymmetry in expression of semaphorin signaling components. (A) *In situ* hybridization demonstrating homogenous distribution of *Polr2a* RNA throughout E15.5 pancreas. (B) *Sema3a* RNA was localized to the mesenchymal periphery of the pancreas. (C) Schematic showing orientation of epithelium, islet cells and mesenchyme. (D,E) Islet cells express Nrp2 at E13.5. (F-I) *Nrp2* is necessary for α cell responses to Sema3a. (J) Quantitative PCR analysis of mRNA expression for plexin A3 in FACS-purified fetal pancreatic cell populations, relative to E15.5 whole pancreas. mRNA of the Nrp2 co-receptor *Plxna3* is enriched in Neurog3^{gfp}-positive fetal islet cells at E15.5 (P=0.03, two tailed t-test versus EpCAM$^+$ epithelial cells, n=4 biological replicates for each group). White circles indicate bead location. Scale bars: 50 µm. Data are mean±s.e.m.

Development (2017) 144, 3744-3754 doi:10.1242/dev.148684

(Fig. 2D,E). From E15.5 to adult stages, Nrp2 expression was primarily detected in α cells (Fig. S3). Nrp2 was not expressed in endocrine progenitor cells marked by Neurog3^{+} nuclei, suggesting expression is acquired only after differentiation into α or β cells (Fig. S3). Nrp1 was not detectable in fetal islet cells, but was present in other pancreatic cell types (Fig. S3). Human fetal α cells expressed NRP2, whereas somatostatin-expressing δ cells expressed NRP1, indicating some signaling features are conserved in human pancreas development (Fig. S3). Upon implanting Sema3a-soaked beads in cultured *Nrp2* knockout mouse pancreas, we did not detect α cell aggregation around beads (Fig. 2F-I). Thus, Nrp2 is required for islet cell responses to Sema3a. These findings also indicate that other receptors like Nrp1 did not compensate for Nrp2 loss, as observed in other systems (Takashima et al., 2002).

Neuropilins act as co-receptors with plexin proteins (Takahashi et al., 1999; Tamagnone et al., 1999). Multiple mRNAs encoding plexins were detected in E15.5 mouse fetal pancreas by RT-PCR (Fig. S3). Assessment of mRNA expression of selected plexin co-receptors in FACS-purified cell populations from the E15.5 pancreas detected enrichment of *Plxna3* in fetal endocrine cells relative to whole pancreas, pancreatic epithelial cell (EpCAM^{+}), or endothelial cell subsets (CD31^{+}; Fig. 2J). Plexins B1 and B2 were expressed in the pancreas, but were not similarly enriched in islet cells (Fig. S3). These data indicate that the expected neuropilin co-receptors are present in the appropriate cell types in the pancreas to facilitate responses to semaphorin cues. Together these findings suggest that semaphorin signals from distal mesenchyme to central Nrp2^{+} islet cells could define an endogenous long-range developmental axis.

Nrp2 is required for islet morphogenesis

Semaphorin guidance signals can be repulsive or attractive, depending on the cellular context (Tran et al., 2007). Based on islet cell attraction to Sema3a-soaked beads and the radially asymmetric distribution of *Sema3a* and *Sema3d* transcripts, we hypothesized that semaphorins function as a chemoattractant cue for developing islet cells. If so, loss of Nrp2 should impair islet cell migration outward from their origin in the central ductal epithelium. To test this hypothesis, we assessed islet development in mice with homozygous inactivation of *Nrp2* (Giger et al., 2000). Because of high-frequency perinatal mortality in homozygous *Nrp2* mutants (Giger et al., 2000), we focused our analysis of pancreas development at E15.5 and postnatal day 1 (P1). At E15.5, islet cells in control littermates were distributed throughout the pancreas as discrete clusters or single islet cells, corresponding to nascent islets and cells migrating to join islets (Fig. 3A). By contrast, in E15.5 *Nrp2* mutants, islet cells formed long streams of hormone^{+} cells along ducts (Fig. 3B). In controls at P1, islets formed as rounded structures distributed throughout the pancreas, with β cells in the islet interior surrounded by α cells (Fig. 3C). In *Nrp2* mutants, we observed abnormal islet cell aggregates enveloping ductal structures in central regions of the pancreas (Fig. 3D,F). Within these aggregates, typical islet architecture appeared preserved, but individual islets were abnormally clustered near other islets and ducts. The ductal and acinar tissue in *Nrp2* mutants appeared similar to controls.

To quantify these phenotypes, we measured specific features of islet development and morphogenesis. Islet α cell and β cell quantities were not detectably altered in *Nrp2* mutants at P1 (P=0.32, α cells; P=0.28, β cells; Fig. 3G), suggesting islet morphogenetic defects did not reflect altered proliferation or differentiation. Measurement of the distance from islets to the nearest ductal structure marked by DBA lectin indicated a 40% reduction in duct-to-islet distance in *Nrp2* mutants at P1 (P=0.03, Fig. 3H). Subsequent analysis of rare surviving adult *Nrp2*-knockout mice indicated that this islet phenotype persisted in adults, with a halving of duct-islet distance detected (P=0.04, Fig. 3H and Fig. S4). We also quantified the extent of contact between ducts and islets and noted a significant increase in islet contact with ductal surfaces in *Nrp2* mutants (97°±2 in controls, 147°±6 in mutants: $P=2\times10^{-5}$, Fig. 3I). Total encirclement of ducts by islets occurred rarely in controls (1.8%) compared with islets in *Nrp2* mutants (8.5%, P=0.0009, Fisher's exact test). Thus, islet separation from ducts appeared to be impaired in *Nrp2* mutants. We did not detect obvious alterations in islet vascularization or innervation in *Nrp2* mutants (Fig. S4). To assess the requirement for *Nrp2* specifically in the pancreatic islets, we attempted conditional inactivation of Nrp2 using a Cre-Lox approach. We did not observe a reduction of Nrp2 expression by immunofluorescence using either Neurog3-Cre or Pdx1-Cre (Fig. S4). Collectively, the phenotypes observed support the view that radial migration of islet cells away from their ductal origin was impaired in *Nrp2* mutants.

Imaging islets in the intact pancreas of *Nrp2* mutants using CLARITY

Prior studies of islet morphogenesis have been limited to reconstruction of three-dimensional islet phenotypes from two-dimensional imaging. To characterize islet developmental defects in the intact pancreas of *Nrp2* mutants at P1, we performed whole-organ confocal imaging using CLARITY (Chung et al., 2013; Tomer et al., 2014). This method permits optical clearing of large tissues while preserving protein and nucleic acid localization, enabling phenotyping of intact organs with cellular resolution. After clearing the pancreas at P1, we assessed islet hormones and ductal markers by immunofluorescence in *Nrp2* wild-type and knockout mice. In controls, islets formed as round clusters distributed both near to and remote from the central ductal network (Fig. 4A,C,E,F; Movie 1). In contrast, islet cells in *Nrp2* knockout mice grew in streams along large central ductal structures (Fig. 4B,D,G,H; Movie 2). Thus, whole-organ imaging of intact pancreata corroborated the morphometric quantification of islet distribution we obtained with sectioned tissue, and supported a model in which Nrp2 signaling is essential for separation and dispersion of islets from their ductal origin during development.

Defective cell migration and deformation in endocrine cells lacking Nrp2

Our analysis of fixed tissues suggested that semaphorin-Nrp2 signaling is essential for migration of developing pancreatic endocrine cells. To test this hypothesis directly, we used live cell imaging to quantify movement and cell shape changes in fetal islet cells (Pauerstein et al., 2015). We used mice harboring a *Neurog3*-tdTomato transgene, which labels all Neurog3^{+} endocrine progenitors and their hormone-expressing progeny (Sugiyama et al., 2013). Time lapse confocal imaging of cultured E13.5 *Nrp2*$^{+/+}$; *Neurog3*-tdTomato control organs for 24 h revealed extensive migration and deformation of developing endocrine cells, including extension of filopodia (Fig. 5A,B,E-H; Movie 3). In contrast, movement of *Neurog3*-tdTomato^{+} cells in *Nrp2* mutants was limited, and these cells failed to undergo deformation (Fig. 5C, D,I-L; Movie 4). Mutant islet cells often remained rounded and near their origin throughout imaging, and many cells did not extend detectable filopodia (Fig. 5E-L; Movie 4). Quantification of cell displacement confirmed a reduction in total distance traveled by single islet cells in *Nrp2* mutants ($P=2\times10^{-11}$; Fig. 5M, Fig. S5). Measurement of total cell shape change during imaging confirmed a

Development (2017) 144, 3744-3754 doi:10.1242/dev.148684

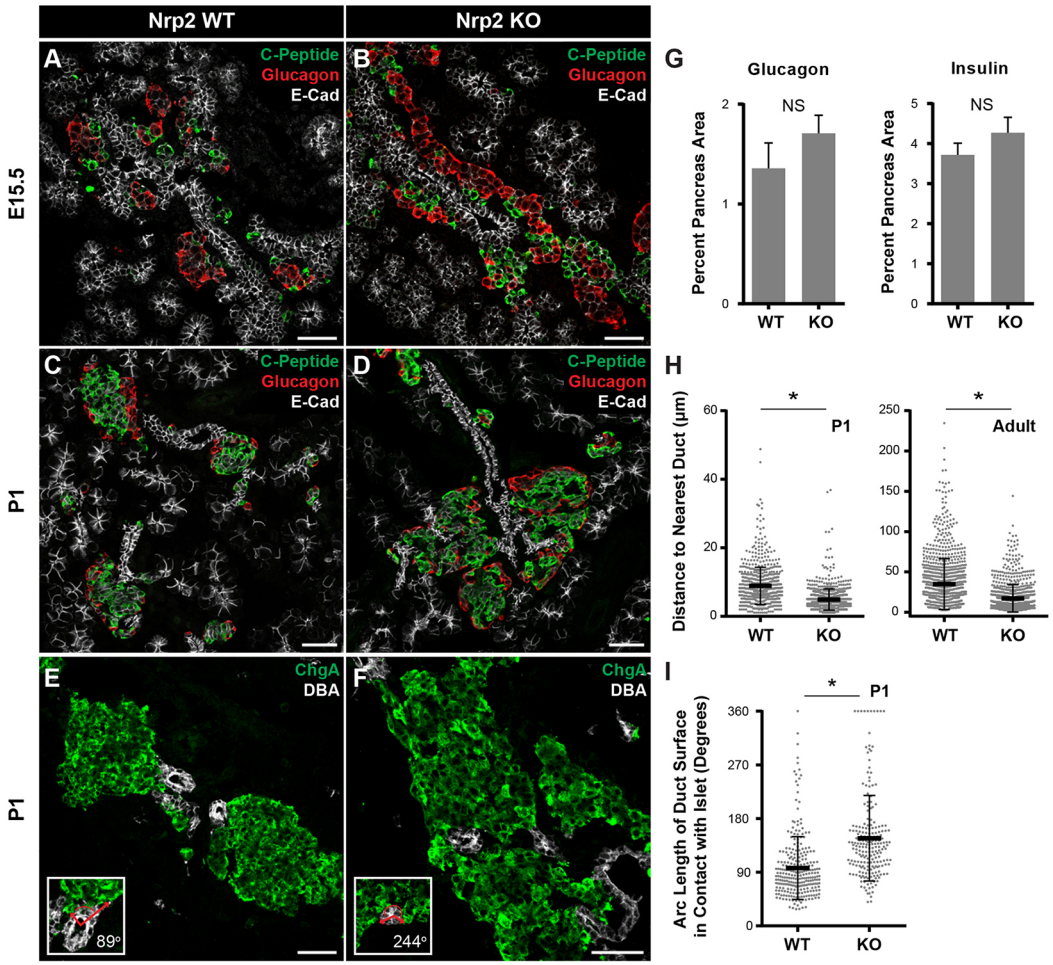

Fig. 3. Nrp2 is necessary for islet morphogenesis. (A,B) At E15.5, control islet cells are arranged in small clusters, whereas streams of islet cells are detected parallel to ducts in *Nrp2* knockouts. (C-F) Islets in control P1 pancreas are round and distinct from ducts, but islets in *Nrp2* knockouts surround ducts and form large islet cell aggregates. (G) The sizes of Islet α and β cell areas are unchanged in *Nrp2* knockouts at P1 (P=0.32 for glucagon, P=0.28 for insulin; mean±s.e.m.). (H) Duct-islet distances are reduced in *Nrp2* knockouts at P1 (P=0.026) and in 6-month-old adults (*P=0.04, data are mean±s.d.). (I) Increased contact between ductal basal surfaces and islets in *Nrp2* knockouts (*P=2×10^{-5}, data are mean±s.d.). For all quantification at P1 (H,I), n=6 for wild type and n=4 for knockout; for adult (H), n=4 for wild type and n=3 for knockout. Statistical significance was assessed using a two-tailed t-test. Insets in E,F are examples of quantification in I. Scale bars: 50 μm. Data are mean±s.d.

significant reduction of cell deformation (P=0.003, Fig. 5N). These experiments indicate that Nrp2 is required for fetal islet cell migration and deformation, including cell biological processes such as the filopodia extension that is integral to migration, and provide a cellular mechanism linking defective Nrp2 signaling to defects in islet morphogenesis.

DISCUSSION

We used classical organ culture and genetics to identify mesenchyme-derived cues influencing islet development, and found that semaphorins are unrecognized chemoattractants for α and β cells. Purified Sema3a was sufficient to redirect fetal α and β cell migration toward beads, indicating that semaphorin signaling provides instructive, not merely permissive, cues to these islet cells. Spatially localized production of Sema3a or other semaphorins by peripheral mesenchymal cells could provide instructive cues to guide radial migration of Nrp2^{+} islet cells (Fig. 6). Consistent with this model, loss of Nrp2, a receptor for secreted semaphorins, resulted in impaired cell migration and defects in islet morphogenesis. Thus, our findings suggest that semaphorins are potent long-range chemoattractants for fetal α and β cells, defining a radial axis that controls islet morphogenesis at both unicellular and multicellular levels. To our knowledge, long-range or spatially localized guidance cues coordinating islet morphogenesis have not previously been identified. Future studies, perhaps using conditional genetics in specific cell subsets, could assess the principal semaphorins responsible for regulating islet morphogenesis. Our data raise the likelihood that multiple semaphorins, including Sema3a and Sema3d, could serve this function.

While Sema3a stimulated migration of both fetal α and β cells, this effect appeared more pronounced with α cells. We also found differences in Nrp2 expression between α and β cells: fetal α cell Nrp2 expression was durable and persisted in adult α cells, unlike in β cells, which showed only transient fetal-stage expression. To the extent that Nrp2 appears to be essential for Sema-mediated signaling in fetal islets, our findings raise the possibility that Sema-Nrp2 signaling primarily guides α cell migration and initial β cell migration. In the later stages of islet morphogenesis, it is possible that α cells then influence β cell migration through cues yet to be identified. Our findings also suggest possible functions for Nrp2 signaling in adult islet α cells. These models could be tested by conditional inactivation of Nrp2 in fetal or adult α cells, though we

Development (2017) 144, 3744-3754 doi:10.1242/dev.148684

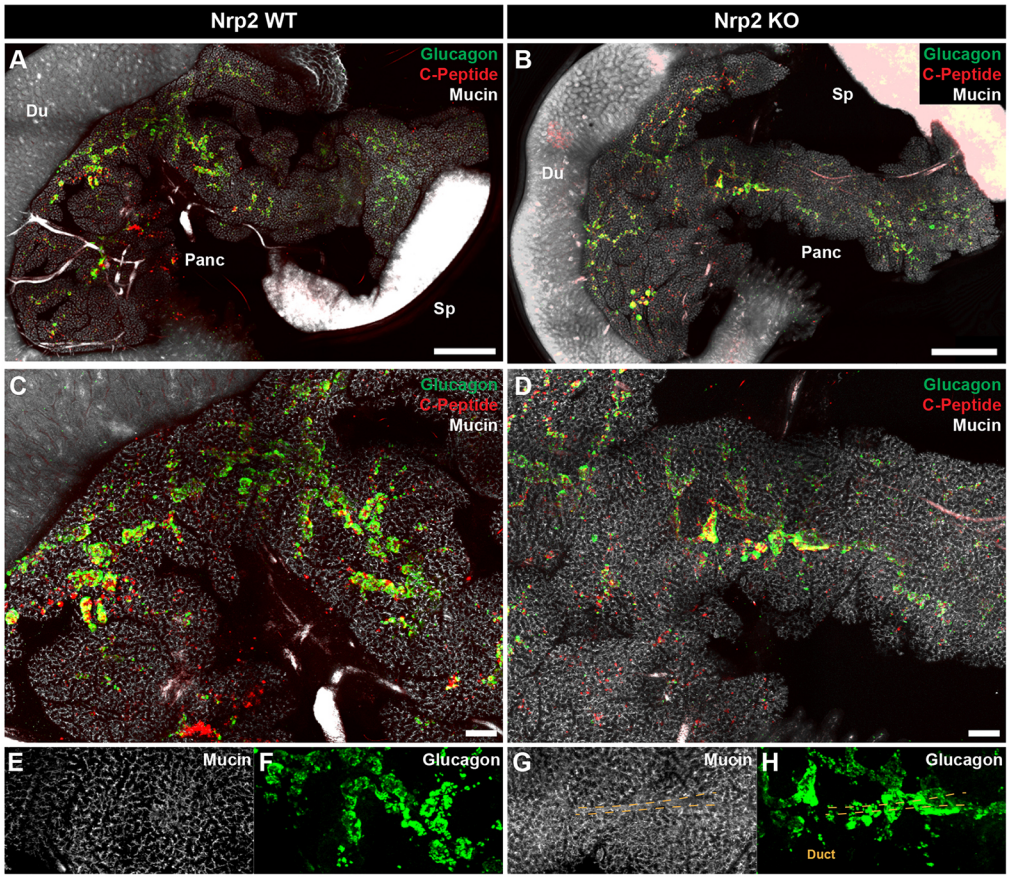

Fig. 4. Whole-organ imaging to assess islet morphology in *Nrp2* knockouts using CLARITY. (A,B) Visualization of islet morphogenesis defects at P1 in three dimensions in the intact pancreas by confocal imaging. Du, duodenum; Sp, spleen; Panc, pancreas. (C,D) Control islets are rounded and begin to form distinct structures at P1, whereas *Nrp2* knockout islet cells form continuous streams along ductal structures. (E-H) Higher magnification views of CLARITY images showing a large ductal structure in a knockout (G) surrounded by a continuous mass of endocrine cells (H, arrowheads and dashed lines indicate example duct structures surrounded by islets). Compare with corresponding regions of control pancreas (E,F). Scale bars: 1 mm in A,B; 200 µm in C,D.

found that the extant conditional 'floxed' *Nrp2*^{f} allele (Walz et al., 2002) was resistant to inactivation by Cre recombinase transgenes, including *Pdx1-Cre* or *Ngn3-Cre*. These have been used previously to inactivate other floxed alleles in the pancreas or fetal islets (Goodyer et al., 2012; Gu et al., 2002). Thus, alternative approaches, perhaps including the generation of additional *Nrp2*^{f} alleles, may be required to pursue conditional genetics in the pancreas.

Semaphorin signaling through Nrp-plexin receptors can be transduced through multiple intracellular pathways that regulate cytoskeletal dynamics leading to oriented cell movement, including Rho GTPases, the Ras pathway or via Cdk5 signaling (Ahmed and Eickholt, 2007; Eickholt et al., 2002; Takahashi et al., 1999). Our preliminary data support a role for Nrp2 signaling through Cdk5 and Rho intermediaries in semaphorin-induced migration of nascent islet cells (P.T.P., K.T. and S.K.K., unpublished). In addition to Sema3a signaling through plexin receptors to cytoskeleton effector proteins, it is also possible that Sema3a signaling leads to an interaction between Nrp2 and integrins to affect cell migration. Nrp2 interactions with integrins at focal adhesions within the same cell (cis) permit integrin binding to laminin in the extracellular matrix, whereas Nrp2 binding to integrins on endothelial cells (trans) allows cancer cell intravasation and extravasation; both of these processes lead to an increase in cancer cell migration or metastasis and poor prognosis (Goel et al., 2012; Cao et al., 2013). Considering that many cancer mechanisms have been adapted from normal developmental events, it is conceivable that such a mechanism might also occur in normal islet morphogenesis.

Distribution of the islets of Langerhans throughout the exocrine tissue is a cardinal pancreatic feature in most vertebrates – including fish, birds, snakes, rodents and primates – suggesting selective forces have maintained this anatomy (Conlon et al., 1988; Moscona, 1990; Steiner et al., 2010). Thus, islet morphogenesis and dispersion is likely controlled by multiple conserved mechanisms. Initially, islet progenitor cells within the fetal ductal epithelium delaminate and, while differentiating, migrate into nascent islet clusters. Multicellular clusters enlarge, reflecting continued cell aggregation and proliferation, and at later fetal and postnatal stages islet cells rearrange to form morphologically mature islets dispersed throughout the exocrine pancreas (Benitez et al., 2012). Our analysis of *Nrp2* mutant mice suggests that the initial differentiation, delamination and clustering of islet cells do not require Sema-Nrp signaling. However, in Nrp2 mutants, islet cells failed to establish normal dispersed islet morphology, leading to abnormally large islet cell aggregates surrounding and connected to major ducts. We postulate that normal islet dispersion could reflect the combination of at least two distinct processes: (1) active directional islet cell migration mediated by a combination of long- and short-range cues, both attractive and repulsive; and (2) growth of intervening non-islet tissues, most abundantly acinar and ductal cells. Other signals are likely involved in islet dispersion: we identified multiple candidate signaling pathways with effects on islet cell development in our screen. However, we focused on semaphorin signaling because of the observed phenotypes in our assays and the availability of reagents to perturb the semaphorin pathway in the pancreas. As pancreatic growth was not detectably impaired in *Nrp2* mutants at birth, tissue growth is likely not sufficient to disperse islets during embryogenesis. In an evolutionary context, the arrangement of islet cells contiguous with their originating epithelium observed in *Nrp2* mutants is reminiscent of findings from jawless fish, where cells expressing pancreatic hormones such as insulin, pancreatic polypeptide and

Development (2017) 144, 3744-3754 doi:10.1242/dev.148684

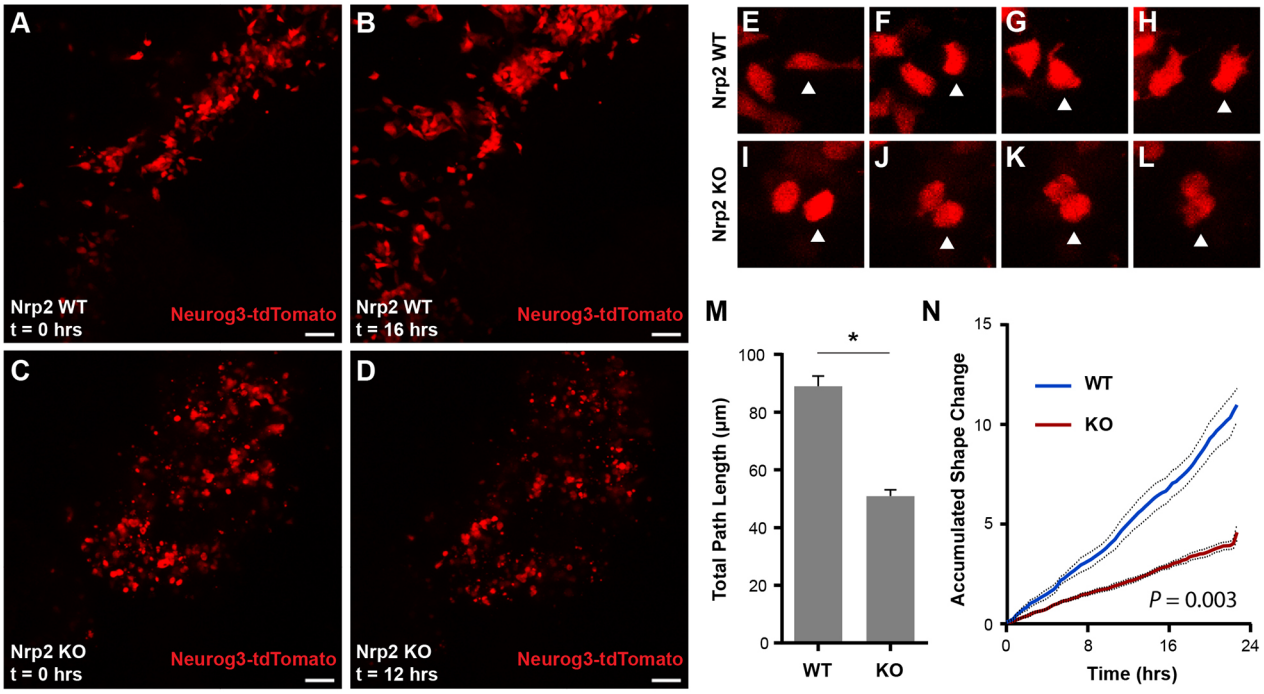

Fig. 5. Loss of *Nrp2* results in defective cell deformation and migration during islet development. (A,B) Frames from time-lapse confocal imaging of Neurog3-tdTomato cells in *Nrp2* wild-type organ cultures. Fetal islet cells undergo deformation, migration and clustering over the 24 h imaging experiment. (C,D) *Nrp2* knockout islet cells fail to undergo normal cell deformation and migration. (E-L) Time-lapse images of single-cell deformation phenotypes in *Nrp2* wild-type and knockout cells. Note deformation and extension of cell processes in E,G,H. Arrowheads indicate one cell tracked over time for each genotype. (M) Quantification of total distance traveled by individual *Nrp2* wild-type and knockout cells (*P=2×10^{-11}). (N) Quantification of cell shape changes over time in *Nrp2* knockout cells (P=0.003, two-tailed *t*-test). Scale bars: 50 μm. Data are mean±s.e.m. Data points were from 38 wild-type and 25 knockout cells, using videos from two separate experiments.

glucagon are found adjacent to or within homologous foregut intestinal epithelium (Conlon et al., 1988; Falkmer, 1979).

The sharing of genetic or signaling modules used to build morphologically or phylogenetically disparate features has been called ‘deep homology’ (Shubin et al., 1997, 2009). Unexpectedly, we found that key elements of a radially oriented signaling pathway regulating cortical lamination in central nervous system development are also deployed for dispersion of islets during pancreas development.

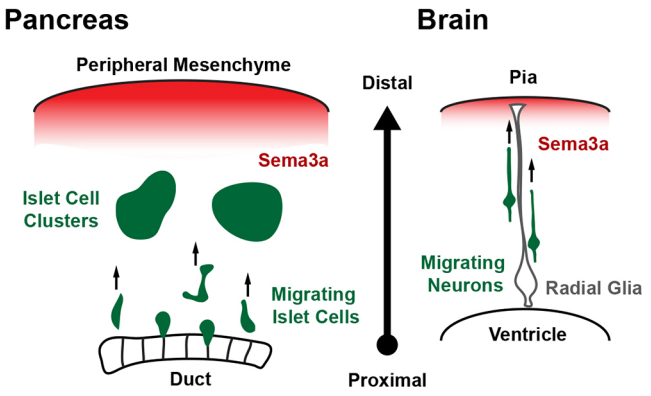

Fig. 6. Model for semaphorin signaling in islet cell radial migration. In the developing pancreas, semaphorin 3a emanates from the peripheral mesenchyme and acts as a chemoattractant for islet cells expressing the semaphorin receptor Nrp2. This signal directs islet cell migration away from their birthplaces in the central ducts and towards the periphery, where they cluster to form islets. Sema3a plays a similar role as a guidance cue in cortical development. There, a peripheral Sema3a signal induces neuropilin- and plexin-dependent radial migration of developing neurons away from the ventricles and towards the pial surface of the cortex.

During mammalian brain development, a stereotyped laminar organization of neurons in the cortex is essential for cortical function. In mice, semaphorins at the distal pial surface signal to postmitotic neurons derived from proximal ventricular zone neural stem cells, directing radial migration toward the pial surface along radial glial cells as cortical lamination proceeds (Chen et al., 2008). In that context, plexin receptors signal through Rho GTPases to direct cell migration towards outer cortical layers (Azzarelli et al., 2014; Pacary et al., 2013). Signaling via Cdk5 also controls multiple aspects of neuronal radial migration and cortical lamination (Chae et al., 1997; Su and Tsai, 2011). Ectopic Sema3a or loss of *Nrp1* is sufficient to disrupt development of this layering. Thus, cortical lamination and pancreatic islet morphogenesis appear to share strikingly similar signaling molecules, cellular processes and developmental axis arrangement (Fig. 6). Sema3a signaling in brain cortical lamination may extend up to several hundred micrometers, comparable with or longer than the distances involved in mouse islet development. Our findings also support prior work that revealed striking similarities between mammalian islet cells and neurons (Ohta et al., 2011; Rulifson et al., 2002; Van Noorden and Falkmer, 1980). As in nervous system development, additional signals conveying chemoattractive, chemorepulsive or ‘stop’ cues might influence islet development. We speculate that an undetected radial or laminar patterning of islets may be linked to specialized functions, responsiveness or control. Consistent with this notion is the observation that human islet inflammation, destruction or preservation in type 1 diabetes mellitus may occur in a heterogeneous pattern (Gaglia et al., 2015; In’t Veld, 2014; Poudel et al., 2015), and that autonomic nerves link groups of islets (Reinert et al., 2014; P.T.P., B.H., K.D. and S.K.K., unpublished).

Discovery of a long-range islet chemoattractant could also influence regenerative approaches to islet reconstitution. In

Development (2017) 144, 3744-3754 doi:10.1242/dev.148684

hematopoietic stem cell transplantation, chemokine-guided migration of stem cells to developmental niches illustrates the therapeutic applications of cellular homing (Copelan, 2006). We speculate that studies of islet guidance cues might help establish similar homing and engraftment paradigms for islet cells or their progenitors.

MATERIALS AND METHODS

Animals

All animal experiments were conducted in accordance with Stanford University IACUC guidelines. Mouse Insulin1 promoter-GFP transgenic mice were purchased from Jackson Laboratories (Hara et al., 2003) and maintained on a CD1 genetic background. Nrp1 floxed (Gu et al., 2003) and Nrp2 knockout mice (Giger et al., 2000) were obtained with permission from Dr David Ginty (Harvard Medical School, Boston, MA, USA) and maintained on a Black6 background. Neurog3-tdTomato transgenic mice have been previously reported and were maintained on a CD1 background (Sugiyama et al., 2013), as were Sema3d$^{GFP\text{-}Cre}$ knock-in mice (Katz et al., 2012). Neurog3$^{gfp/+}$ mice were obtained from Klaus Kaestner (University of Pennsylvania, USA) and maintained on a CD1 background (Lee et al., 2002). Wnt1-Cre (Danielian et al., 1998; Lewis et al., 2013) and Rosa-mTmG (Muzumdar et al., 2007) mice were obtained from the Jackson Laboratories and maintained on a mixed Black6 and CD1 background. Transgenic Ngn3-Cre and Pdx1-Cre mice have been previously described (Gu et al., 2002). Floxed Nrp2 mice (Walz et al., 2002) were obtained from the Kolodkin lab (Johns Hopkins School of Medicine and HHMI, MD, USA) and maintained by the Epstein and Kim labs. Experiments and morphometry analysis were performed on mice at embryonic day (E) 13.5, E15.5, postnatal day 1 and 6 months; both male and female mice were used in all experiments.

Organ culture and live imaging

For organ culture experiments, fetal pancreatic rudiments were dissected from E13.5 mouse embryos, embedded in type 1 collagen gel (EMD Millipore) and cultured in DMEM/F12 supplemented with 10% fetal bovine serum and 1% penicillin/streptomycin for experiments not involving beads (Gittes et al., 1996; Puri and Hebrok, 2007). The FBS concentration was reduced to 0.5% for bead assays in the screen. Medium was changed every other day for experiments not involving beads. For bead assays, one half of the media volume was refreshed daily for the duration of experiments. Organs were fixed in 4% PFA and then processed for whole-mount immunofluorescence or for cryosectioning.

For live-imaging experiments, E13.5 organs were dissected and visually assessed for transgene presence. For Nrp2 knockout experiments, rapid genotyping was performed using the Phire Tissue Direct kit (Thermo Fisher). Samples were mounted in type 1 collagen gel (EMD Millipore) in glass-bottomed dishes (MatTek) and cultured in organ culture media without Phenol Red (described above) supplemented with 1% insulin-transferrin-selenium. Images were acquired using a Leica SP8 inverted confocal system equipped with a white light laser and an environmental control chamber using a 20× water immersion objective. For detection of tdTomato, samples were excited at 561 nm. Images were acquired at 20 min intervals for all time-lapse experiments. Data were saved in LIF format and analyzed using Volocity image analysis software (Perkin Elmer) or ImageJ. Quantification of cell shape changes have been described elsewhere (Pauerstein et al., 2015). Cell displacement and velocity measurements were calculated using the MTrackJ plugin in ImageJ (Meijering et al., 2012).

Bead screen

Affi-Gel Blue beads, 100-200 mesh (Bio Rad 153-7302), were incubated in 100 ng/ml growth factor overnight at 4°C. Beads were washed in sterile PBS before implanting into mouse fetal organ culture in three locations: one in the ventral pancreas, one in the proximal region of the dorsal pancreas and one in the distal region of the dorsal pancreas. For screening, bright-field and GFP images were acquired at days 1 and 5 using a Leica MZ16FA stereomicroscope, with a constant exposure time and total magnification of 50× maintained for all assays. Images were opened in ImageJ (Schneider et al., 2012) and *Ins1*-GFP intensity as a function of radius was calculated using the 'Radial Profile' plug-in. Images were converted to grayscale, the center of the bead was defined by the user and intensity was calculated from r=0 pixels to r=250 pixels (325 µm) using the 'Radial Profile' tool. Only beads in the proximal dorsal pancreas were assessed for calculating shift values, because of the favorable optical properties of the tissue in that region. Results tables relating radius and GFP intensity were exported to custom templates in Microsoft Excel, in which the formula:

$$x = 0.5 \times \sum_{r=0}^{r=325} \frac{GFP\ Intensity(r)}{Circumference(r)}$$

was used to calculate mean radial positions corresponding to the weighted centers of intensity plots. *GFP Intensity* (*r*) refers to the sum of pixel intensity values along the circle defined by the radius *r* from the center of the bead, and *Circumference* (*r*) refers to the circumference of that circle. Weighted centers of intensity at day 0 were subtracted from values at day 5 for each individual pancreas to generate 'shift' values, which describe changes in overall β cell distribution around beads: $Shift = x_{day\ 5} - x_{day\ 0}$. Negative shift values indicate an attractive effect on β cells, whereas positive shift values indicate a repulsive effect. Shift values were calculated for three to seven organs per candidate signal, averaged and compared with PBS control bead assays using a two-tailed Student's *t*-test. *P* values less than 0.05 were considered significant. Growth factors used are indicated in Table S1. Chemical inhibitors used are indicated in Table S2.

Immunostaining

Tissue was fixed in 4% PFA overnight and processed for cryosectioning. Samples were blocked in 1% BSA and 0.2% nonfat evaporated milk supplemented with 0.5% Triton X-100 and 1% DMSO, and antibody incubations were performed in blocking buffer. AlexaFluor- and Dylight-conjugated secondary antibodies (Life Technologies and Jackson Immunoresearch) were used for detection. Antibodies used are indicated in Table S3.

For all morphometric analyses, images representing entire pancreatic sections were acquired using a Zeiss AxioM1 microscope. At least 12 sections of 10 µm thickness and separated by at least 120 µm were analyzed for each organ. For quantification of α and β cell areas, tissue was immunostained for E-Cadherin and appropriate hormone markers. E-Cadherin-positive areas were manually traced in ImageJ, and images were thresholded to calculate hormone-positive areas using the 'Analyze Particles' function. Total hormone$^+$ areas were divided by total E-Cadherin$^+$ areas for each biological sample. For duct-islet distance measurements, tissue was labeled using DBA lectin and antibodies to ChgA. Distances from ChgA$^+$ islet edges to nearest DBA lectin$^+$ structure were measured using the 'Line' function in ImageJ. All islet clusters larger than 4 cells were measured in all sections analyzed for each pancreas. For assessment of duct contact with islets, ducts cut in cross-section and adjacent to islets were visually identified. The ImageJ 'Angle' tool was used to measure the angle defined by the center of the duct and the two edges of islet contact with the basal surface of the duct. Data were exported to Microsoft Excel and Graphpad Prism for analysis. Distance or angle measurements were averaged for each independent sample, and biological groups were compared using statistical methods described below. Measurements were performed by individuals blinded to the genotypes of samples.

CLARITY methods

Whole organ analysis of pancreatic islet morphology was performed using CLARITY (Chung et al., 2013; Hsueh et al., 2017) with several modifications. Tissue was dissected in ice-cold PBS and immediately incubated in hydrogel monomer solution for 3-5 days at 4°C. The hydrogel monomer solution is 4% PFA, 4% acrylamide, 0.25% VA-044 initiator and 0.05% saponin in PBS. Bis-acrylamide, included in the original formulation (Chung et al., 2013), was omitted to prevent polymerization of hydrogel outside the tissue. Tissue was cleared passively for 5-14 days by incubating in clearing buffer (4% SDS, 200 mM boric acid at pH 8.5) at 55°C (Tomer et al., 2014). After clearing, tissue was washed in PBS and immunostained using standard protocols, with antibody incubations extended to 3-5 days to permit penetration of thick samples. Samples were mounted in FocusClear

Development (2017) 144, 3744-3754 doi:10.1242/dev.148684

(CelExplorer Labs) and imaged using an Olympus confocal microscope equipped with 5× air and 10× water immersion objectives. Tiled *z*-stack datasets were stitched into a single *z*-stack using Fiji (Schindelin et al., 2012) and were visualized using Volocity image analysis software. 3D reconstruction videos were created using Arivis Vision4D software.

FACS and gene expression measurement

Pancreatic rudiments were dissected from E15.5 embryos and processed as previously described (Sugiyama et al., 2007), with the exception that organs were dissociated using Accutase (eBioscience). Single-cell suspensions were stained using antibodies described in Table S1 and were sorted using a BD FACS Aria II. Red blood cells were depleted from the cell fractions using RBC lysis buffer (BioLegend). Cells were collected in PBS supplemented with 2% BSA and 10 mM EGTA. RNA was purified using the PicoPure RNA extraction system (Life Technologies), cDNA was synthesized using Superscript III reverse transcriptase (Life Technologies), and gene expression was measured using qPCR with Taqman probes and an ABI7500 qPCR system (Applied Biosystems).

For analysis of plexin gene expression in FACS-purified cell populations, E15.5 Neurog3$^{gfp/+}$ pancreas was obtained and processed for FACS as above, with fractions defined as follows: GFP^{+}CD133^{low}EpCAM$^{low/neg}$CD31^{-} cells were considered to be 'endocrine', EpCAM^{+}GFP^{-} cells were 'EpCAM', CD31^{+}GFP^{-}EpCAM^{-} cells were 'CD31' and EpCAM^{-}GFP^{-}CD31^{-} cells were considered 'Negative' and represent a mixed population of cells not encompassed by the other cell fractions (Benitez et al., 2014; Sugiyama et al., 2007). CD45^{+} white blood cells were excluded from all fractions, and red blood cells were depleted as described above.

Gene expression analysis using quantitative RT-PCR was performed using the following Taqman probes (Life Technologies): *Sema3a*, Mm00436469; *Sema3d*, Mm01224783; *Pecam*, Mm01242584; *S100a4*, Mm00803372; vimentin, Mm01333430; *Acta2*, Mm00725412; *Syp*, Mm00436850; *Sox9*, Mm00448840; *Ins2*, Mm00731595; *Plxna3*, Mm00501170; *Plxnb1*, Mm00555359; and *Plxnb2*, Mm00507118.

To assess plexin family gene expression by RT-PCR, RNA was isolated from microdissected whole E15.5 wild-type mouse pancreas (CD1 background) using the PicoPure RNA Isolation Kit (Life Technologies). cDNA was synthesized using Superscript III reverse transcriptase, and gene expression was assessed by PCR using BioMix Red (Bioline) and the primer sets indicated in Table S4.

In situ hybridization

RNA *in situ* hybridization was performed using the RNAscope system (Advanced Cell Diagnostics, ACD). Probes for mouse *Sema3a* (ACD 412961) and *Polr2a* (ACD 312471) were purchased from ACD, as were RNAscope 2.0 (Brown reagents). For fluorescence detection, tyramide signal amplification reagents (Life Technologies) were used in place of DAB reagents. *In situ* hybridizations were performed on freshly sectioned cryoembedded tissue samples at stages indicated in the text.

Human tissue samples

Experiments involving human tissue samples were approved by the Stanford University School of Medicine Institutional Review Board. Human pancreatic tissue between gestational days (GD) 75 and 110 was obtained through the Birth Defects Research Laboratory, University of Washington (Seattle, WA, USA). All donors provided informed consent.

Statistical analysis

Data are presented as mean±s.e.m. unless otherwise indicated. Student's *t*-test was used for statistical comparisons unless otherwise noted. *P* values less than 0.05 were considered significant. Statistical analysis was performed using Graphpad Prism and Microsoft Excel software.

Acknowledgements

We thank members of the Kim Lab for helpful discussion and advice, Dr Jon Mulholland and Kitty Lee of the Stanford Cell Sciences Imaging Facility for assistance with confocal microscopy, and Drs P. Lwigale (Rice University), M. Scott (Stanford University) and R. Nusse (Stanford University) for sharing reagents.

Competing interests

The authors declare no competing or financial interests.

Author contributions

Conceptualization: P.T.P., S.K.K.; Methodology: P.T.P., K.T., K.B.W., K.M.P., B.H., J.A.E., S.K.K.; Validation: P.T.P., K.T., K.M.P., B.H., S.K.K.; Formal analysis: P.T.P., K.T., K.B.W., K.M.P., B.H., X.G.; Investigation: P.T.P., K.T., K.B.W., K.M.P., B.H., H.E.A., X.G., H.A., K.D., S.K.K.; Resources: H.A., K.D., J.A.E., S.K.K.; Data curation: P.T.P.; Writing - original draft: P.T.P., S.K.K.; Writing - review & editing: P.T.P., K.T., K.B.W., K.M.P., B.H., H.A., K.D., J.A.E., S.K.K.; Visualization: P.T.P., K.T., B.H.; Supervision: K.D., J.A.E., S.K.K.; Project administration: S.K.K.; Funding acquisition: S.K.K.

Funding

P.T.P. was supported by the Howard Hughes Medical Institute Medical Fellows program, the Stanford Medical Scientist Training Program and by the National Institutes of Health (F30DK102301). K.T. was supported by a National Science Foundation graduate research fellowship (DGE-114747). H.E.A. was supported by a Juvenile Diabetes Research Foundation postdoctoral fellowship. J.A.E. is supported by the National Institutes of Health (HL118768). Work in the Kim lab was supported by the Howard Hughes Medical Institute, Juvenile Diabetes Research Foundation, the Leona M. and Harry B. Helmsley Charitable Trust, and the H. L. Snyder Medical Foundation. Deposited in PMC for release after 6 months.

Supplementary information

Supplementary information available online at
http://dev.biologists.org/lookup/doi/10.1242/dev.148684.supplemental

References

Acloque, H., Adams, M. S., Fishwick, K., Bronner-Fraser, M. and Nieto, M. A. (2009). Epithelial-mesenchymal transitions: the importance of changing cell state in development and disease. *J. Clin. Invest.* **119**, 1438-1449.

Afelik, S., Qu, X., Hasrouni, E., Bukys, M. A., Deering, T., Nieuwoudt, S., Rogers, W., MacDonald, R. J. and Jensen, J. (2012). Notch-mediated patterning and cell fate allocation of pancreatic progenitor cells. *Development* **139**, 1744-1753.

Ahmed, A. and Eickholt, B. J. (2007). Intracellular kinases in semaphorin signaling. *Adv. Exp. Med. Biol.* **600**, 24-37.

Anderson, K. R., Singer, R. A., Balderes, D. A., Hernandez-Lagunas, L., Johnson, C. W., Artinger, K. B. and Sussel, L. (2011). The L6 domain tetraspanin Tm4sf4 regulates endocrine pancreas differentiation and directed cell migration. *Development* **138**, 3213-3224.

Apelqvist, A., Li, H., Sommer, L., Beatus, P., Anderson, D. J., Honjo, T., Hrabe de Angelis, M., Lendahl, U. and Edlund, H. (1999). Notch signalling controls pancreatic cell differentiation. *Nature* **400**, 877-881.

Azzarelli, R., Pacary, E., Garg, R., Garcez, P., van den Berg, D., Riou, P., Ridley, A. J., Friedel, R. H., Parsons, M. and Guillemot, F. (2014). An antagonistic interaction between PlexinB2 and Rnd3 controls RhoA activity and cortical neuron migration. *Nat. Commun.* **5**, 3405.

Benitez, C. M., Goodyer, W. R. and Kim, S. K. (2012). Deconstructing pancreas developmental biology. *Cold Spring Harb. Perspect. Biol.* **4**, a012401.

Benitez, C. M., Qu, K., Sugiyama, T., Pauerstein, P. T., Liu, Y., Tsai, J., Gu, X., Ghodasara, A., Arda, H. E., Zhang, J. et al. (2014). An integrated cell purification and genomics strategy reveals multiple regulators of pancreas development. *PLoS Genet.* **10**, e1004645.

Bhushan, A., Itoh, N., Kato, S., Thiery, J. P., Czernichow, P., Bellusci, S. and Scharfmann, R. (2001). Fgf10 is essential for maintaining the proliferative capacity of epithelial progenitor cells during early pancreatic organogenesis. *Development* **128**, 5109-5117.

Blum, B., Roose, A. N., Barrandon, O., Maehr, R., Arvanites, A. C., Davidow, L. S., Davis, J. C., Peterson, Q. P., Rubin, L. L. and Melton, D. A. (2014). Reversal of β cell de-differentiation by a small molecule inhibitor of the TGFβ pathway. *eLife* **3**, e02809

Brissova, M., Shostak, A., Shiota, M., Wiebe, P. O., Poffenberger, G., Kantz, J., Chen, Z., Carr, C., Jerome, W. G., Chen, J. et al. (2006). Pancreatic islet production of vascular endothelial growth Factor-A is essential for islet vascularization, revascularization, and function. *Diabetes* **55**, 2974-2985.

Cai, Q., Brissova, M., Reinert, R. B., Cheng Pan, F., Brahmachary, P., Jeansson, M., Shostak, A., Radhika, A., Poffenberger, G., Quaggin, S. E. et al. (2012). Enhanced expression of VEGF-A in β cells increases endothelial cell number but impairs islet morphogenesis and β cell proliferation. *Dev. Biol.* **367**, 40-54.

Cao, Y., Hoeppner, L. H., Bach, S. E. G., Guo, Y., Wang, E., Wu, J., Cowley, M. J., Chang, D. K., Waddell, N. et al. (2013). Neuropilin-2 promotes extravasation and metastasis by interacting with endothelial α5 integrin. *Cancer Res.* **73**, 4579-4590.

Chae, T., Kwon, Y. T., Bronson, R., Dikkes, P., Li, E. and Tsai, L.-H. (1997). Mice lacking p35, a neuronal specific activator of Cdk5, display cortical lamination defects, seizures, and adult lethality. *Neuron* **18**, 29-42.

Chen, H., Chédotal, A., He, Z., Goodman, C. S. and Tessier-Lavigne, M. (1997). Neuropilin-2, a novel member of the neuropilin family, is a high affinity receptor for the semaphorins Sema E and Sema IV but not Sema III. *Neuron* **19**, 547-559.
Chen, G., Sima, J., Jin, M., Wang, K.-Y., Xue, X.-J., Zheng, W., Ding, Y.-Q. and Yuan, X.-B. (2008). Semaphorin-3A guides radial migration of cortical neurons during development. *Nat. Neurosci.* **11**, 36-44.
Chen, H., Gu, X., Liu, Y., Wang, J., Wirt, S. E., Bottino, R., Schorle, H., Sage, J. and Kim, S. K. (2011). PDGF signalling controls age-dependent proliferation in pancreatic β-cells. *Nature* **478**, 349-355.
Chung, K., Wallace, J., Kim, S.-Y., Kalyanasundaram, S., Andalman, A. S., Davidson, T. J., Mirzabekov, J. J., Zalocusky, K. A., Mattis, J., Denisin, A. K. et al. (2013). Structural and molecular interrogation of intact biological systems. *Nature* **497**, 332-337.
Cleaver, O. and Dor, Y. (2012). Vascular instruction of pancreas development. *Development* **139**, 2833-2843.
Cohen, T., Herzog, Y., Brodzky, A., Greenson, J. K., Eldar, S., Gluzman-Poltorak, Z., Neufeld, G. and Resnick, M. B. (2002). Neuropilin-2 is a novel marker expressed in pancreatic islet cells and endocrine pancreatic tumours. *J. Pathol.* **198**, 77-82.
Conlon, J. M., Reinecke, M., Thorndyke, M. C. and Falkmer, S. (1988). Insulin and other islet hormones (somatostatin, glucagon and PP) in the neuroendocrine system of some lower vertebrates and that of invertebrates–a minireview. *Horm. Metab. Res. Horm. Stoffwechselforschung Horm. Métabolisme* **20**, 406-410.
Copelan, E. A. (2006). Hematopoietic stem-cell transplantation. *N. Engl. J. Med.* **354**, 1813-1826.
Cras-Méneur, C., Li, L., Kopan, R. and Permutt, M. A. (2009). Presenilins, Notch dose control the fate of pancreatic endocrine progenitors during a narrow developmental window. *Genes Dev.* **23**, 2088-2101.
Danielian, P. S., Muccino, D., Rowitch, D. H., Michael, S. K. and McMahon, A. P. (1998). Modification of gene activity in mouse embryos in utero by a tamoxifen-inducible form of Cre recombinase. *Curr. Biol. CB* **8**, 1323-1326.
Degenhardt, K., Singh, M. K., Aghajanian, H., Massera, D., Wang, Q., Li, J., Li, L., Choi, C., Yzaguirre, A. D., Francey, L. J. et al. (2013). Semaphorin 3d signaling defects are associated with anomalous pulmonary venous connections. *Nat. Med.* **19**, 760-765.
Eickholt, B. J., Walsh, F. S. and Doherty, P. (2002). An inactive pool of GSK-3 at the leading edge of growth cones is implicated in Semaphorin 3A signaling. *J. Cell Biol.* **157**, 211-217.
Epstein, J. A., Aghajanian, H. and Singh, M. K. (2015). Semaphorin signaling in cardiovascular development. *Cell Metab.* **21**, 163-173.
Esni, F., Ghosh, B., Biankin, A. V., Lin, J. W., Albert, M. A., Yu, X., MacDonald, R. J., Civin, C. I., Real, F. X., Pack, M. A. et al. (2004). Notch inhibits Ptf1 function and acinar cell differentiation in developing mouse and zebrafish pancreas. *Development* **131**, 4213-4224.
Falkmer, S. (1979). Immunocytochemical studies of the evolution of islet hormones. *J. Histochem. Cytochem. Off. J. Histochem. Soc.* **27**, 1281-1282.
Fukuda, T., Takeda, S., Xu, R., Ochi, H., Sunamura, S., Sato, T., Shibata, S., Yoshida, Y., Gu, Z., Kimura, A. et al. (2013). Sema3A regulates bone-mass accrual through sensory innervations. *Nature* **497**, 490-493.
Gaglia, J. L., Harisinghani, M., Aganj, I., Wojtkiewicz, G. R., Hedgire, S., Benoist, C., Mathis, D. and Weissleder, R. (2015). Noninvasive mapping of pancreatic inflammation in recent-onset type-1 diabetes patients. *Proc. Natl. Acad. Sci. USA* **112**, 2139-2144.
Giger, R. J., Cloutier, J.-F., Sahay, A., Prinjha, R. K., Levengood, D. V., Moore, S. E., Pickering, S., Simmons, D., Rastan, S., Walsh, F. S. et al. (2000). Neuropilin-2 is required in vivo for selective axon guidance responses to secreted semaphorins. *Neuron* **25**, 29-41.
Gittes, G. K. (2009). Developmental biology of the pancreas: a comprehensive review. *Dev. Biol.* **326**, 4-35.
Gittes, G. K., Galante, P. E., Hanahan, D., Rutter, W. J. and Debase, H. T. (1996). Lineage-specific morphogenesis in the developing pancreas: role of mesenchymal factors. *Development* **122**, 439-447.
Goel, H. L., Pursell, B., Standley, C., Fogarty, K. and Mercurio, A. (2012). Neuropilin-2 regulates α6β1 integrin in the formation of focal adhesions and signaling. *J. Cell Sci.* **125**, 497-506.
Golosow, N. and Grobstein, C. (1962). Epitheliomesenchymal interaction in pancreatic morphogenesis. *Dev. Biol.* **4**, 242-255.
Goodyer, W. R., Gu, X., Liu, Y., Bottino, R., Crabtree, G. R. and Kim, S. K. (2012). Neonatal β cell development in mice and humans is regulated by calcineurin/NFAT. *Dev. Cell* **23**, 21-34.
Gouzi, M., Kim, Y. H., Katsumoto, K., Johansson, K. and Grapin-Botton, A. (2011). Neurogenin3 initiates stepwise delamination of differentiating endocrine cells during pancreas development. *Dev. Dyn. Off. Publ. Am. Assoc. Anat.* **240**, 589-604.
Greiner, T. U., Kesavan, G., Ståhlberg, A. and Semb, H. (2009). Rac1 regulates pancreatic islet morphogenesis. *BMC Dev. Biol.* **9**, 2.
Gu, G., Dubauskaite, J. and Melton, D. A. (2002). Direct evidence for the pancreatic lineage: NGN3+ cells are islet progenitors and are distinct from duct progenitors. *Development* **129**, 2447-2457.
Gu, C., Rodriguez, E. R., Reimert, D. V., Shu, T., Fritzsch, B., Richards, L. J., Kolodkin, A. L. and Ginty, D. D. (2003). Neuropilin-1 conveys semaphorin and VEGF signaling during neural and cardiovascular development. *Dev. Cell* **5**, 45-57.
Guo, T., Landsman, L., Li, N. and Hebrok, M. (2013). Factors expressed by murine embryonic pancreatic mesenchyme enhance generation of insulin-producing cells from hESCs. *Diabetes* **62**, 1581-1592.
Hara, M., Wang, X., Kawamura, T., Bindokas, V. P., Dizon, R. F., Alcoser, S. Y., Magnuson, M. A. and Bell, G. I. (2003). Transgenic mice with green fluorescent protein-labeled pancreatic β-cells. *Am. J. Physiol. Endocrinol. Metab.* **284**, E177-E183.
Hsueh, B., Burns, V. M., Pauerstein, P., Holzem, K., Ye, L., Engberg, K., Wang, A.-C., Gu, X., Chakravarthy, H., Arda, H. E. et al. (2017). Pathways to clinical CLARITY: volumetric analysis of irregular, soft, and heterogeneous tissues in development and disease. *Sci. Rep.* **7**, 5899.
Ieda, M., Kanazawa, H., Kimura, K., Hattori, F., Ieda, Y., Taniguchi, M., Lee, J.-K., Matsumura, K., Tomita, Y., Miyoshi, S. et al. (2007). Sema3a maintains normal heart rhythm through sympathetic innervation patterning. *Nat. Med.* **13**, 604-612.
In't Veld, P. (2014). Insulitis in human type 1 diabetes: a comparison between patients and animal models. *Semin. Immunopathol.* **36**, 569-579.
Katz, T. C., Singh, M. K., Degenhardt, K., Rivera-Feliciano, J., Johnson, R. L., Epstein, J. A. and Tabin, C. J. (2012). Distinct compartments of the proepicardial organ give rise to coronary vascular endothelial cells. *Dev. Cell* **22**, 639-650.
Kesavan, G., Lieven, O., Mamidi, A., Öhlin, Z. L., Johansson, J. K., Li, W.-C., Lommel, S., Greiner, T. U. and Semb, H. (2014). Cdc42/N-WASP signaling links actin dynamics to pancreatic β cell delamination and differentiation. *Development* **141**, 685-696.
Kim, S. K. and Hebrok, M. (2001). Intercellular signals regulating pancreas development and function. *Genes Dev.* **15**, 111-127.
Kolodkin, A. L., Matthes, D. J. and Goodman, C. S. (1993). The semaphorin genes encode a family of transmembrane and secreted growth cone guidance molecules. *Cell* **75**, 1389-1399.
Kolodkin, A. L., Levengood, D. V., Rowe, E. G., Tai, Y.-T., Giger, R. J. and Ginty, D. D. (1997). Neuropilin is a semaphorin III receptor. *Cell* **90**, 753-762.
Konstantinova, I., Nikolova, G., Ohara-Imaizumi, M., Meda, P., Kucˇera, T., Zarbalis, K., Wurst, W., Nagamatsu, S. and Lammert, E. (2007). EphA-Ephrin-A-mediated beta cell communication regulates insulin secretion from pancreatic islets. *Cell* **129**, 359-370.
Lammert, E., Cleaver, O. and Melton, D. (2001). Induction of pancreatic differentiation by signals from blood vessels. *Science* **294**, 564-567.
Lammert, E., Gu, G., McLaughlin, M., Brown, D., Brekken, R., Murtaugh, L. C., Gerber, H.-P., Ferrara, N. and Melton, D. A. (2003). Role of VEGF-A in vascularization of pancreatic islets. *Curr. Biol.* **13**, 1070-1074.
Landsman, L., Nijagal, A., Whitchurch, T. J., Vanderlaan, R. L., Zimmer, W. E., Mackenzie, T. C. and Hebrok, M. (2011). Pancreatic mesenchyme regulates epithelial organogenesis throughout development. *PLoS Biol.* **9**, e1001143.
Lee, C. S., Perreault, N., Brestelli, J. E. and Kaestner, K. H. (2002). Neurogenin 3 is essential for the proper specification of gastric enteroendocrine cells and the maintenance of gastric epithelial cell identity. *Genes Dev.* **16**, 1488-1497.
Lewis, A. E., Vasudevan, H. N., O'Neill, A. K., Soriano, P. and Bush, J. O. (2013). The widely used Wnt1-Cre transgene causes developmental phenotypes by ectopic activation of Wnt signaling. *Dev. Biol.* **379**, 229-234.
Meijering, E., Dzyubachyk, O. and Smal, I. (2012). Methods for cell and particle tracking. *Methods Enzymol.* **504**, 183-200.
Metzger, D. E., Gasperowicz, M., Otto, F., Cross, J. C., Gradwohl, G. and Zaret, K. S. (2012). The transcriptional co-repressor Grg3/Tle3 promotes pancreatic endocrine progenitor delamination and β-cell differentiation. *Development* **139**, 1447-1456.
Miettinen, P. J., Huotari, M., Koivisto, T., Ustinov, J., Palgi, J., Rasilainen, S., Lehtonen, E., Keski-Oja, J. and Otonkoski, T. (2000). Impaired migration and delayed differentiation of pancreatic islet cells in mice lacking EGF-receptors. *Development* **127**, 2617-2627.
Miralles, F., Battelino, T., Czernichow, P. and Scharfmann, R. (1998). TGF-beta plays a key role in morphogenesis of the pancreatic islets of Langerhans by controlling the activity of the matrix metalloproteinase MMP-2. *J. Cell Biol.* **143**, 827-836.
Moscona, A. A. (1990). Anatomy of the pancreas and Langerhans islets in snakes and lizards. *Anat. Rec.* **227**, 232-244.
Muñoz-Bravo, J. L., Hidalgo-Figueroa, M., Pascual, A., López-Barneo, J., Leal-Cerro, A. and Cano, D. A. (2013). GDNF is required for neural colonization of the pancreas. *Development* **140**, 3669-3679.
Murtaugh, L. C., Stanger, B. Z., Kwan, K. M. and Melton, D. A. (2003). Notch signaling controls multiple steps of pancreatic differentiation. *Proc. Natl. Acad. Sci. USA* **100**, 14920-14925.
Muzumdar, M. D., Tasic, B., Miyamichi, K., Li, L. and Luo, L. (2007). A global double-fluorescent Cre reporter mouse. *Genes. N. Y. N 2000* **45**, 593-605.
Ohta, Y., Kosaka, Y., Kishimoto, N., Wang, J., Smith, S. B., Honig, G., Kim, H., Gasa, R. M., Neubauer, N., Liou, A. et al. (2011). Convergence of the insulin and serotonin programs in the pancreatic β-cell. *Diabetes* **60**, 3208-3216.

Pacary, E., Azzarelli, R. and Guillemot, F. (2013). Rnd3 coordinates early steps of cortical neurogenesis through actin-dependent and -independent mechanisms. *Nat. Commun.* **4**, 1635.
Pagliuca, F. W., Millman, J. R., Gürtler, M., Segel, M., Van Dervort, A., Ryu, J. H., Peterson, Q. P., Greiner, D. and Melton, D. A. (2014). Generation of functional human pancreatic β cells in vitro. *Cell* **159**, 428-439.
Pauerstein, P. T., Sugiyama, T., Stanley, S. E., McLean, G. W., Wang, J., Martín, M. G. and Kim, S. K. (2015). Dissecting human gene functions regulating islet development with targeted gene transduction. *Diabetes* **64**, 3037-3049.
Polleux, F., Giger, R. J., Ginty, D. D., Kolodkin, A. L. and Ghosh, A. (1998). Patterning of cortical efferent projections by semaphorin-neuropilin interactions. *Science* **282**, 1904-1906.
Poudel, A., Savari, O., Striegel, D. A., Periwal, V., Taxy, J., Millis, J. M., Witkowski, P., Atkinson, M. A. and Hara, M. (2015). Beta-cell destruction and preservation in childhood and adult onset type 1 diabetes. *Endocrine* **49**, 693-702.
Puri, S. and Hebrok, M. (2007). Dynamics of embryonic pancreas development using real-time imaging. *Dev. Biol.* **306**, 82-93.
Puri, S. and Hebrok, M. (2010). Cellular plasticity within the pancreas–lessons learned from development. *Dev. Cell* **18**, 342-356.
Reinert, R. B., Brissova, M., Shostak, A., Pan, F. C., Poffenberger, G., Cai, Q., Hundemer, G. L., Kantz, J., Thompson, C. S., Dai, C. et al. (2013). Vascular endothelial growth factor-a and islet vascularization are necessary in developing, but not adult, pancreatic islets. *Diabetes* **62**, 4154-4164.
Reinert, R. B., Cai, Q., Hong, J.-Y., Plank, J. L., Aamodt, K., Prasad, N., Aramandla, R., Dai, C., Levy, S. E., Pozzi, A. et al. (2014). Vascular endothelial growth factor coordinates islet innervation via vascular scaffolding. *Development* **141**, 1480-1491.
Rezania, A., Bruin, J. E., Arora, P., Rubin, A., Batushansky, I., Asadi, A., O'Dwyer, S., Quiskamp, N., Mojibian, M., Albrecht, T. et al. (2014). Reversal of diabetes with insulin-producing cells derived in vitro from human pluripotent stem cells. *Nat. Biotechnol.* **132**, 1121-1133.
Roccisana, J., Reddy, V., Vasavada, R. C., Gonzalez-Pertusa, J. A., Magnuson, M. A. and Garcia-Ocaña, A. (2005). Targeted inactivation of hepatocyte growth factor receptor c-met in beta-cells leads to defective insulin secretion and GLUT-2 downregulation without alteration of beta-cell mass. *Diabetes* **54**, 2090-2102.
Rodriguez-Diaz, R., Dando, R., Jacques-Silva, M. C., Fachado, A., Molina, J., Abdulreda, M. H., Ricordi, C., Roper, S. D., Berggren, P.-O. and Caicedo, A. (2011). Alpha cells secrete acetylcholine as a non-neuronal paracrine signal priming beta cell function in humans. *Nat. Med.* **17**, 888-892.
Rukstalis, J. M. and Habener, J. F. (2007). Snail2, a mediator of epithelial-mesenchymal transitions, expressed in progenitor cells of the developing endocrine pancreas. *Gene Expr. Patterns GEP* **7**, 471-479.
Rulifson, E. J., Kim, S. K. and Nusse, R. (2002). Ablation of insulin-producing neurons in flies: growth and diabetic phenotypes. *Science* **296**, 1118-1120.
Sanvito, F., Herrera, P. L., Huarte, J., Nichols, A., Montesano, R., Orci, L. and Vassalli, J. D. (1994). TGF-beta 1 influences the relative development of the exocrine and endocrine pancreas in vitro. *Development* **120**, 3451-3462.
Schindelin, J., Arganda-Carreras, I., Frise, E., Kaynig, V., Longair, M., Pietzsch, T., Preibisch, S., Rueden, C., Saalfeld, S., Schmid, B. et al. (2012). Fiji: an open-source platform for biological-image analysis. *Nat. Methods* **9**, 676-682.
Schneider, C. A., Rasband, W. S. and Eliceiri, K. W. (2012). NIH Image to ImageJ: 25 years of image analysis. *Nat. Methods* **9**, 671-675.
Serup, P. (2012). Signaling pathways regulating murine pancreatic development. *Semin. Cell Dev. Biol.* **23**, 663-672.
Shelly, M., Cancedda, L., Lim, B. K., Popescu, A. T., Cheng, P., Gao, H. and Poo, M. (2011). Semaphorin3A regulates neuronal polarization by suppressing axon formation and promoting dendrite growth. *Neuron* **71**, 433-446.
Shih, H. P., Kopp, J. L., Sandhu, M., Dubois, C. L., Seymour, P. A., Grapin-Botton, A. and Sander, M. (2012). A Notch-dependent molecular circuitry initiates pancreatic endocrine and ductal cell differentiation. *Development* **139**, 2488-2499.
Shubin, N., Tabin, C. and Carroll, S. (1997). Fossils, genes and the evolution of animal limbs. *Nature* **388**, 639-648.
Shubin, N., Tabin, C. and Carroll, S. (2009). Deep homology and the origins of evolutionary novelty. *Nature* **457**, 818-823.
Steiner, D. J., Kim, A., Miller, K. and Hara, M. (2010). Pancreatic islet plasticity: interspecies comparison of islet architecture and composition. *Islets* **2**, 135-145.
Su, S. C. and Tsai, L.-H. (2011). Cyclin-dependent kinases in brain development and disease. *Annu. Rev. Cell Dev. Biol.* **27**, 465-491.
Sugiyama, T., Rodriguez, R. T., McLean, G. W. and Kim, S. K. (2007). Conserved markers of fetal pancreatic epithelium permit prospective isolation of islet progenitor cells by FACS. *Proc. Natl. Acad. Sci. USA* **104**, 175-180.
Sugiyama, T., Benitez, C. M., Ghodasara, A., Liu, L., McLean, G. W., Lee, J., Blauwkamp, T. A., Nusse, R., Wright, C. V. E., Gu, G. et al. (2013). Reconstituting pancreas development from purified progenitor cells reveals genes essential for islet differentiation. *Proc. Natl. Acad. Sci. USA* **110**, 12691-12696.
Takahashi, T., Fournier, A., Nakamura, F., Wang, L.-H., Murakami, Y., Kalb, R. G., Fujisawa, H. and Strittmatter, S. M. (1999). Plexin-neuropilin-1 complexes form functional semaphorin-3A receptors. *Cell* **99**, 59-69.
Takashima, S., Kitakaze, M., Asakura, M., Asanuma, H., Sanada, S., Tashiro, F., Niwa, H., Miyazaki, J.-I., Hirota, S., Kitamura, Y. et al. (2002). Targeting of both mouse neuropilin-1 and neuropilin-2 genes severely impairs developmental yolk sac and embryonic angiogenesis. *Proc. Natl. Acad. Sci. USA* **99**, 3657-3662.
Tamagnone, L., Artigiani, S., Chen, H., He, Z., Ming, G.-I., Song, H., Chedotal, A., Winberg, M. L., Goodman, C. S., Poo, M. et al. (1999). Plexins are a large family of receptors for transmembrane, secreted, and GPI-anchored semaphorins in vertebrates. *Cell* **99**, 71-80.
Tomer, R., Ye, L., Hsueh, B. and Deisseroth, K. (2014). Advanced CLARITY for rapid and high-resolution imaging of intact tissues. *Nat. Protoc.* **9**, 1682-1697.
Tran, T. S., Kolodkin, A. L. and Bharadwaj, R. (2007). Semaphorin regulation of cellular morphology. *Annu. Rev. Cell Dev. Biol.* **23**, 263-292.
Tran, T. S., Rubio, M. E., Clem, R. L., Johnson, D., Case, L., Tessier-Lavigne, M., Huganir, R. L., Ginty, D. D. and Kolodkin, A. L. (2009). Secreted semaphorins control spine distribution and morphogenesis in the postnatal CNS. *Nature* **462**, 1065-1069.
Tulachan, S. S., Tei, E., Hembree, M., Crisera, C., Prasadan, K., Koizumi, M., Shah, S., Guo, P., Bottinger, E. and Gittes, G. K. (2007). TGF-beta isoform signaling regulates secondary transition and mesenchymal-induced endocrine development in the embryonic mouse pancreas. *Dev. Biol.* **305**, 508-521.
Van der Meulen, T., Donaldson, C. J., Cáceres, E., Hunter, A. E., Cowing-Zitron, C., Pound, L. D., Adams, M. W., Zembrzycki, A., Grove, K. L. and Huising, M. O. (2015). Urocortin3 mediates somatostatin-dependent negative feedback control of insulin secretion. *Nat. Med.* **21**, 769-776.
Van Noorden, S. and Falkmer, S. (1980). Gut-islet endocrinology-some evolutionary aspects. *Invest. Cell Pathol.* **3**, 21-35.
Walz, A., Rodriguez, I. and Mombaerts, P. (2002). Aberrant sensory innervation of the olfactory bulb in neuropilin-2 mutant mice. *J. Neurosci. Off. J. Soc. Neurosci.* **22**, 4025-4035.
Wessells, N. K. and Cohen, J. H. (1967). Early pancreas organogenesis: morphogenesis, tissue interactions, and mass effects. *Dev. Biol.* **15**, 237-270.
Winberg, M. L., Noordermeer, J. N., Tamagnone, L., Comoglio, P. M., Spriggs, M. K., Tessier-Lavigne, M. and Goodman, C. S. (1998). Plexin A is a neuronal semaphorin receptor that controls axon guidance. *Cell* **95**, 903-916.
Yang, Y. H. C., Szabat, M., Bragagnini, C., Kott, K., Helgason, C. D., Hoffman, B. G. and Johnson, J. D. (2011). Paracrine signalling loops in adult human and mouse pancreatic islets: netrins modulate beta cell apoptosis signalling via dependence receptors. *Diabetologia* **54**, 828-842.
Yebra, M., Montgomery, A. M. P., Diaferia, G. R., Kaido, T., Silletti, S., Perez, B., Just, M. L., Hildbrand, S., Hurford, R., Florkiewicz, E. et al. (2003). Recognition of the neural chemoattractant Netrin-1 by integrins alpha6beta4 and alpha3beta1 regulates epithelial cell adhesion and migration. *Dev. Cell* **5**, 695-707.
Yoshitomi, H. and Zaret, K. S. (2004). Endothelial cell interactions initiate dorsal pancreas development by selectively inducing the transcription factor Ptf1a. *Development* **131**, 807-817.

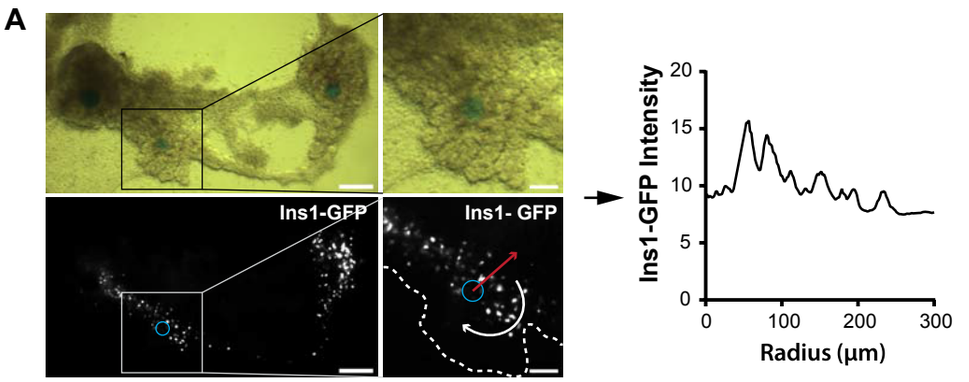

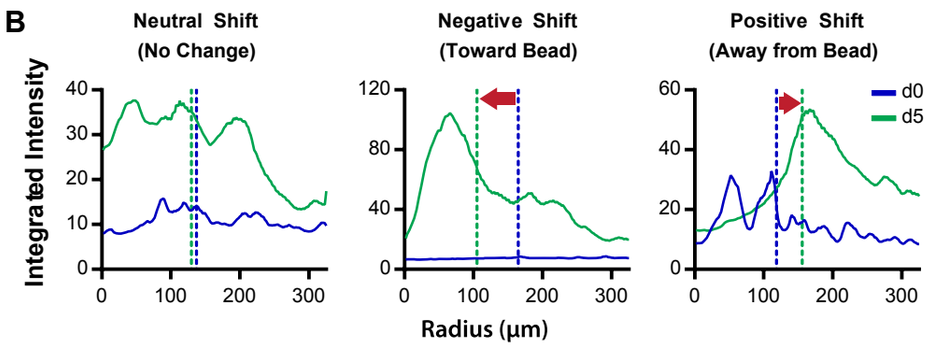

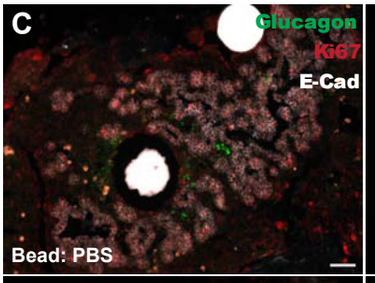

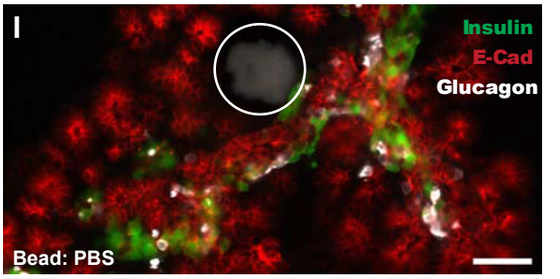

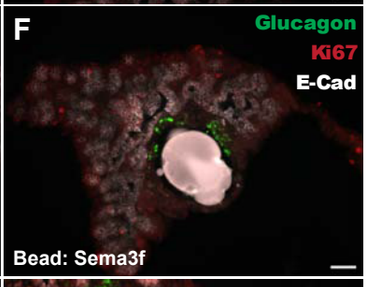

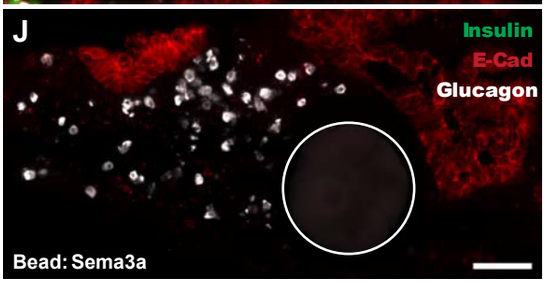

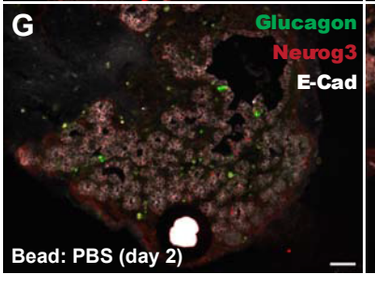

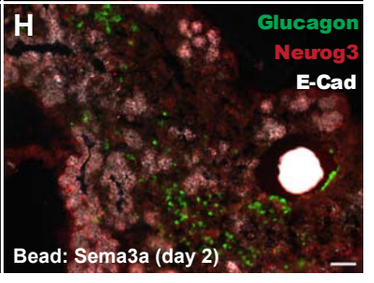

Figure S1. Supplemental data related to bead screen. (A) Description of methods used for screening candidate growth factors and quantifying changes in β cell position over time. Growth factor-soaked agarose beads (blue) were implanted into E13.5 fetal mouse pancreatic organ cultures. *Ins1*-GFP fluorescence was measured as a function of radius from the central bead; lower right fluorescence image indicates measurement of *Ins1*-GFP intensity along a line (red arrow) rotated 360º (white arrow) from the center of the bead (blue circle). Fluorescence intensity was measured along the circumference of each circle with radius from 0 to 325 μm and normalized for path length, with resulting chart indicated at right. (B) Examples of Shift calculations for three organs. Blue line indicates day 0 measurements; green line indicates day 5 measurements. The center of the bead is defined as radius = 0 μm. (C-F) Sema3a, Sema3b, and Sema3f are capable of inducing alpha cell swarming of beads in the distal dorsal pancreas. None induce expression of Ki67 in alpha cells. (G,H) No alteration of islet precursor marker Neurog3 expression with Sema3a bead. (I,J) Alpha cells responding to Sema3a beads invade into mesenchyme and lose E-Cadherin expression. White circles indicate bead placement. Scale bars: 100 μm (A, C-H) and 50 μm (I,J).

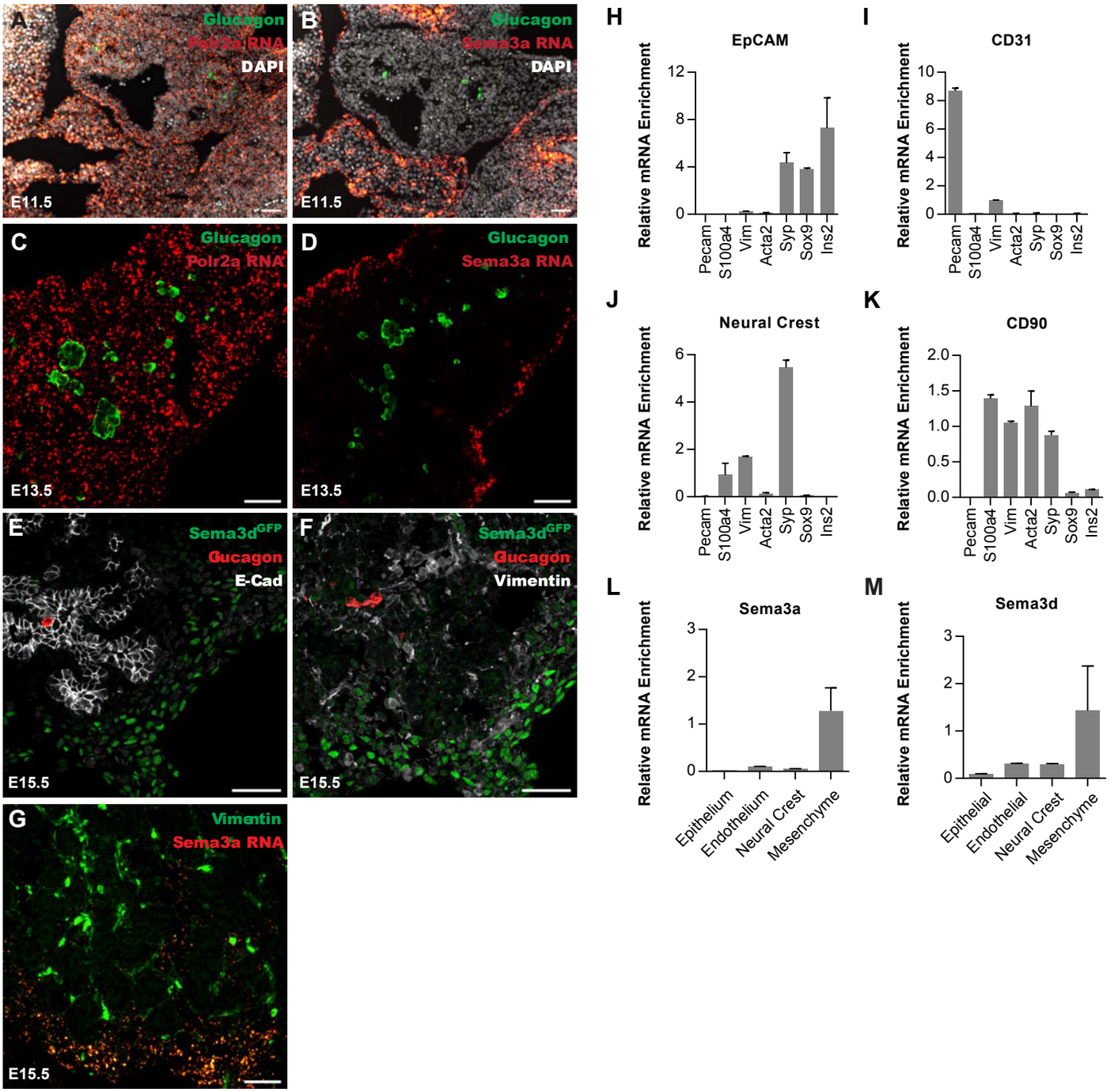

Figure S2. Supplemental data related to Semaphorin expression. (A-D) *Sema3a* mRNA is expressed along the pancreatic periphery at earlier developmental stages, including E11 and E13. (E,F) Expression of Sema3d^{GFP} transgene is restricted to peripheral pancreatic mesenchymal cells. (G) *Sema3a* mRNA expression overlaps with peripheral mesenchymal cells. (L-M) *Sema3a* and *Sema3d* mRNA are enriched in FACS-purified mesenchymal cells; validation of FACS purified cell populations are presented (H-K). Data in (H-M) presented as mean±SEM. Scale bars: 50 μm.

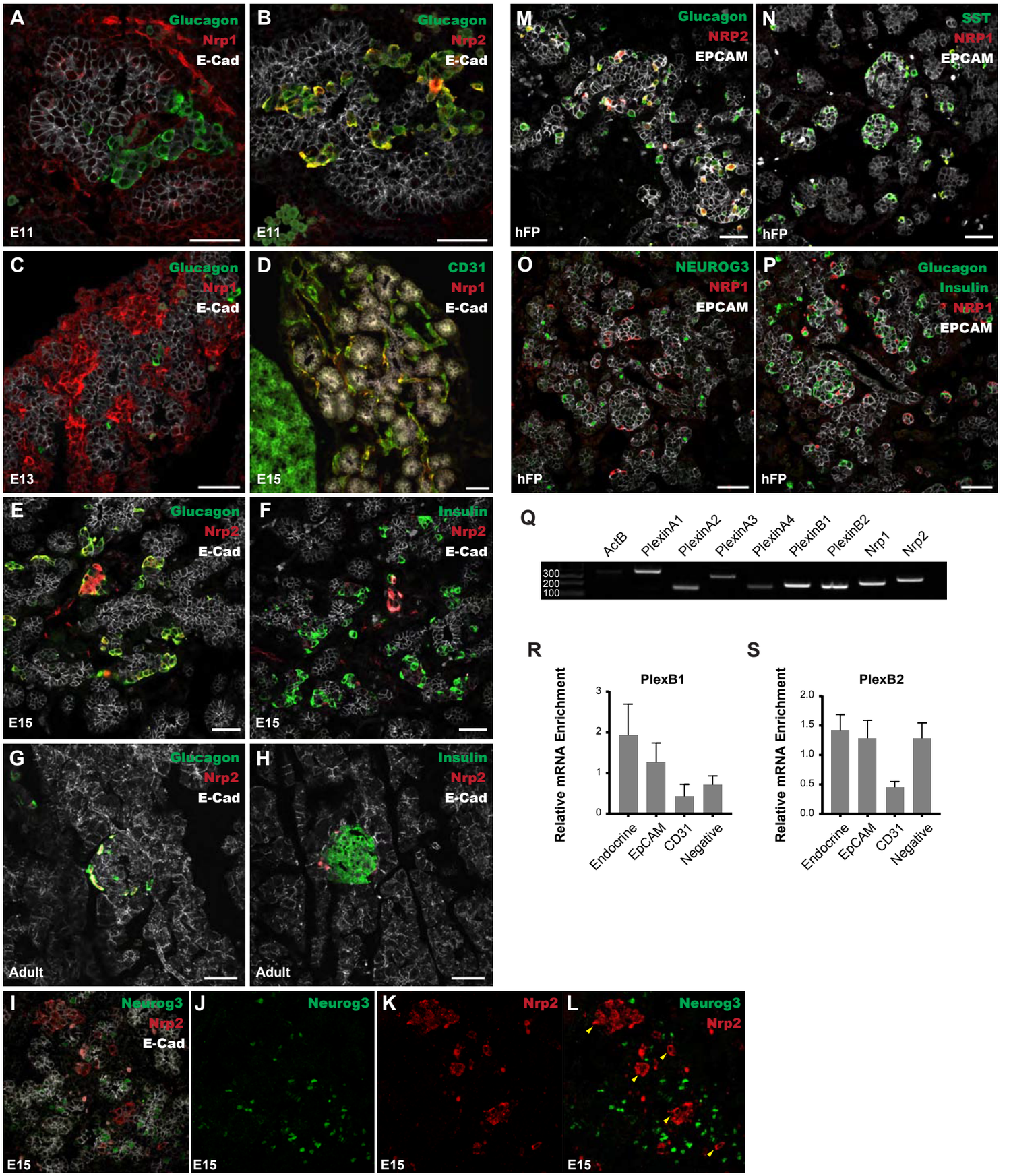

Figure S3. Expression of Semaphorin receptors in the pancreas. (A,B) At E11.5, Nrp1 is expressed within the pancreatic epithelium but not in α cells. Nrp2 is expressed in α cells. (C) Nrp1 is expressed primarily in the mesenchyme at E13.5, and in a subset of epithelial cells. (D) Expression of Nrp1 at E15.5 overlaps with $CD31^+$ endothelial cells. (E-H) Nrp2 is expressed in α cells, but not β cells, at E15.5 and in adult mice. (I-L) Nrp2 is not expressed in islet progenitor cells, marked by Neurogenin 3^+ signal, at e15. (M-P) In the human fetal pancreas, NRP2 is expressed in α cells, and NRP1 is expressed in δ cells. NRP1 is also expressed in a subset of $EPCAM^+$ epithelial cells that does not coexpress NEUROG3, Insulin, or Glucagon. (Q) Expression of Plexin mRNA by RT-PCR in E15.5 pancreas. (R,S) Expression of *PlexinB* genes in FACS-purified cell populations shows a lack of enrichment in islet cells at E15.5 relative to $EpCAM^+$ epithelial cells or whole pancreas. Data presented as mean±SEM. Scale bars: 50 μm.

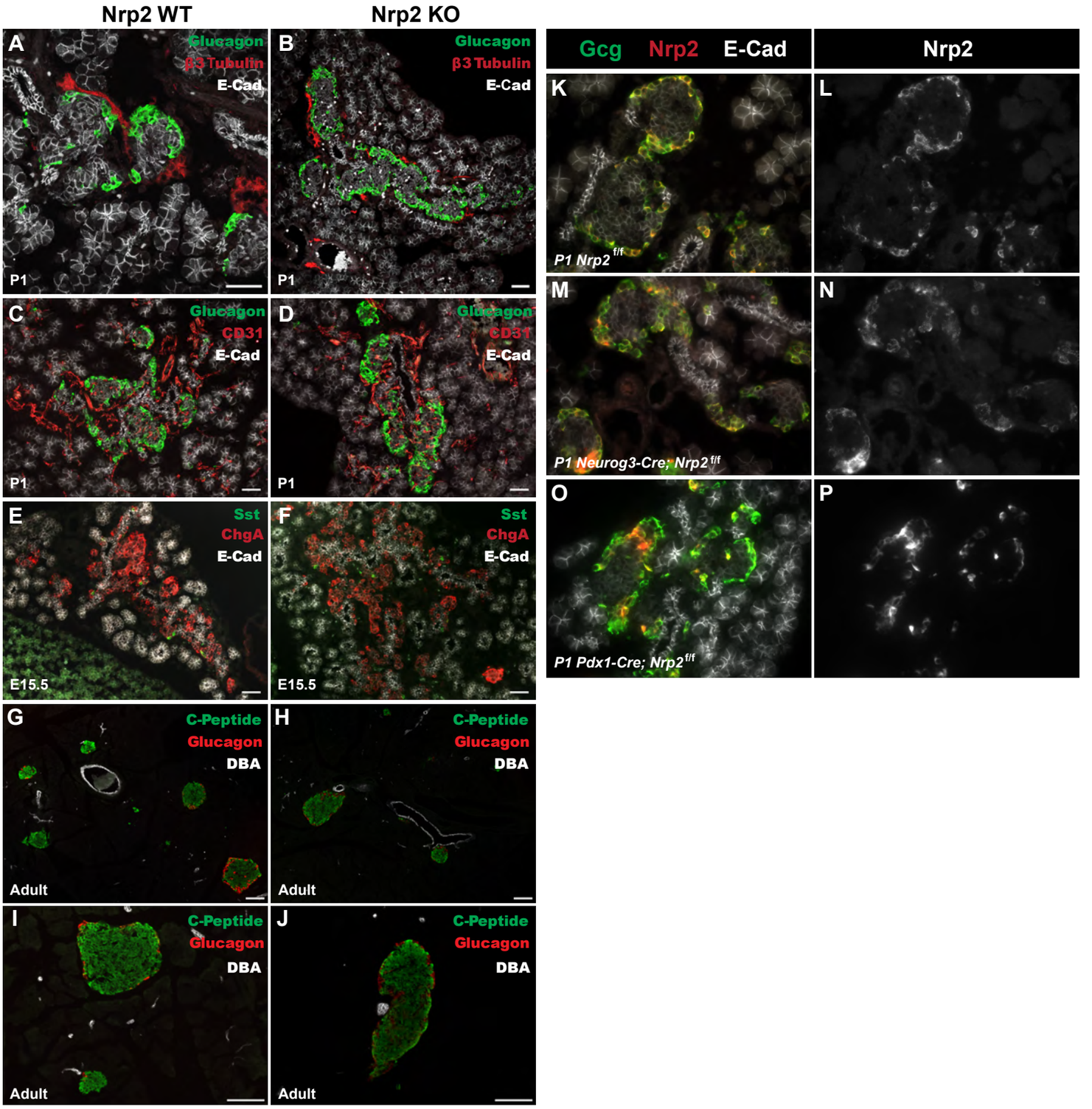

Figure S4. Supplemental data related to *Nrp2* knockout analysis. (A-D) No gross alterations in islet innervation or vascularization at P1. (E,F) No apparent changes in δ cell development at E15.5. (G-J) Islet histology in surviving adult *Nrp2* knockout mice demonstrates islet association with ducts. (K-P) The *Nrp2* floxed allele is not efficiently excised by pancreas specific Ngn3 cre and Pdx1 cre transgenes at P0. Scale bars: 50 μm.

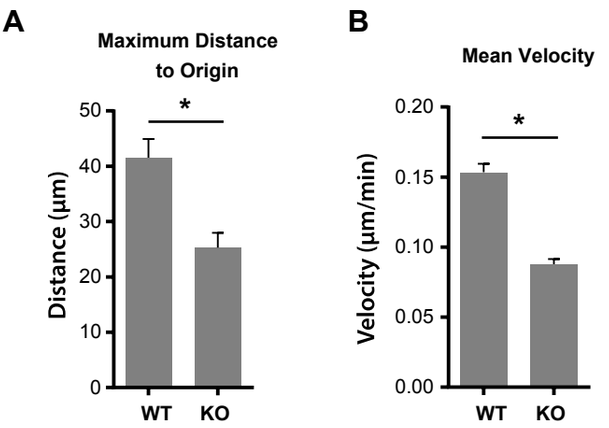

Figure S5. Live imaging analysis supplement. (A) Quantification of maximum distance from cell position at t=0 hrs in live imaging of *Nrp2* wild-type and knockout cells (P=0.001, n = 38 WT and 25 KO). (B) Quantification of mean cell velocity in live imaging (P=2x10^{-11}, n = 38 WT and 25 KO). Both presented as mean ± SEM, P values from two-tailed t-test.

Movie 1. CLARITY 3D reconstruction of *Nrp2* wild type whole pancreas at P1. Islets (glucagon, red; c-peptide, green) in *Nrp2* wild type pancreas form distinct small islet clusters both close and distant to ductal structures (mucin, white). The 3D reconstruction movies were created in Arivis Vision4D software using data from Figure 4.

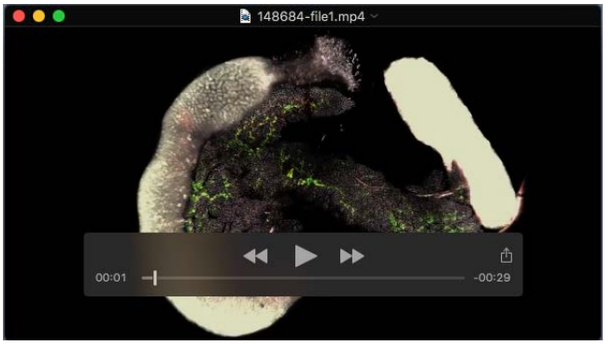

Movie 2. CLARITY 3D reconstruction of *Nrp2* knockout type whole pancreas at P1. Islets (glucagon, red; c-peptide, green) in *Nrp2* knockout type pancreas form distinct small islets clusters, but also form large islet aggregates that are in close proximity to ductal structures (mucin, white). The 3D reconstruction movies were created in Arivis Vision4D software using data from Figure 4.

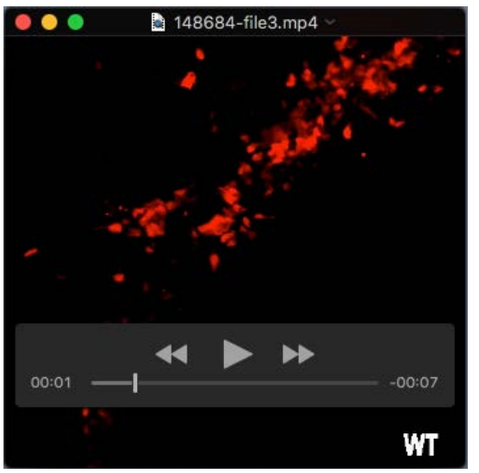

Movie 3. 24 hour time-lapse video of endocrine cell migration and deformation in *Nrp2* wild type embryonic pancreas explant. Endocrine lineage cells (red) in *Nrp2* wild type pancreas ($Nrp2^{+/+}$; Neurog3-tdTomato) readily display cell migration and cell deformation, such as filopodia extensions. Time-lapse video is created from data in Figure 5.

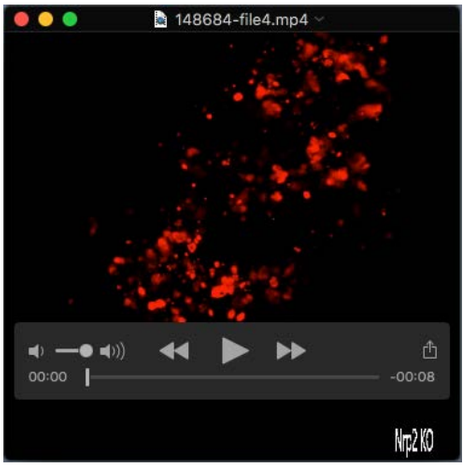

Movie 4. 24 hour time-lapse video of endocrine cell migration and deformation in *Nrp2* knockout embryonic pancreas explant. Endocrine lineage cells (red) in *Nrp2* knockout pancreas ($Nrp2^{-/-}$; Neurog3-tdTomato) show limited migration and cell deformation compared to Nrp2 wild type control (Movie S3). Time-lapse video is created from data in Figure 5.

Supplemental Tables

Table S1. Growth factors used in bead screen

Growth factor	Company	Catalog Number	n (organs in screen)
PDGF-BB (human recombinant)	R&D Systems	220-BB-010	3
BMP4 (human recombinant)	R&D Systems	314-BP-010	6
Noggin (human recombinant)	R&D Systems	6057-NG-025	5
HGF (human recombinant)	R&D Systems	294-HG-005	5
Activin A (human recombinant)	R&D Systems	338-AC-010	5
GDF3 (human recombinant)	R&D Systems	5754-G3-010	7
IGF1 (human recombinant)	R&D Systems	291-G1-200	3
TGFβ1 (human recombinant)	R&D Systems	240-B-002	5
Sema3a (human recombinant, Fc fusion)	R&D Systems	1250-S3-025	6
TGFβ3 (human recombinant)	R&D Systems	243-B3-002	6
VEGF (human recombinant)	Peprotech	AF-100-20A	7
Wnt3a (mouse recombinant)	R&D Systems	1324-WN-002	4
EGF (human recombinant)	Sigma	E9644	4
RSPO1 (human recombinant)	Peprotech	120-38	5
Shh (human recombinant)	Peprotech	315-22	3
Cxcl13 (mouse recombinant)	Peprotech	250-24	4
Cxcl12 (mouse recombinant)	R&D System	460-SD-010	6
Fgf2 (human recombinant)	Peprotech	100-18B	5
Exendin4	Tocris	1933	3
Ang1 (human recombinant)	Peprotech	130-06	3
sFRP1 (human recombinant)	Peprotech	120-29	3
Sema3a (mouse recombinant, Fc fusion)	R&D Systems	5926-S3-025	N/A
Sema3b (mouse recombinant, Fc fusion)	R&D Systems	5440-S3-025	N/A
Sema3f (mouse recombinant, Fc fusion)	R&D Systems	3237-S3-025	N/A

Table S2. Chemical inhibitors			
Inhibitor	**Concentration**	**Company**	**Catalog Number**
CHIR99021 (GSK3 inhibitor)	1 μM	Selleck Chemicals	S2924
LIMKi3 (LIM Kinase inhibitor)	10 μM	EMD Millipore	435930
IPA3 (PAK inhibitor)	10 μM	EMD Millipore	506106
Y-27632 (ROCK inhibitor)	10 μM	EMD Millipore	688000
Roscovitine (CDK5 inhibitor)	10 μM	EMD Millipore	557360

Table S3. Antibodies*				
Antigen	**Antibody type**	**Source**	**Catalog number**	**Dilution**
Insulin	Guinea pig polyclonal	Dako	A0564	500
c-Peptide	Rabbit polyclonal	Cell Signaling Technologies	4593	500
Glucagon	Guinea pig polyclonal	Clontech	M182	5,000
Chromogranin A	Rabbit polyclonal	Immunostar	20085	500
E-Cadherin	Rat monoclonal	Life Technologies	13-1900	500
Mucin	Hamster monoclonal	Thermo Scientific	HM-1630	500
Nrp1	Rabbit monoclonal (EPR3113)	Abcam	ab81321	250
Nrp2	Rabbit monoclonal (D39A5)	Cell Signaling Technologies	3366	250
Vimentin	Rabbit monoclonal (D21H3)	Cell Signaling Technologies	5741	200
PDGFRa	Rabbit monoclonal (D1E1E)	Cell Signaling Technologies	3174	400
CD90 (AF488)	Rat monoclonal (30-H12)	BioLegend	105315	250
EpCAM (Biotin)	Mouse monoclonal (G8.8)	BioLegend	118204	250
CD31 (BV421)	Mouse monoclonal (390)	BioLegend	102423	250
EPCAM	Mouse monoclonal (1B7)	eBioscience	13-9326	250
DBA	*(Dolichos biflorus agglutinin* lectin, biotinylated)	Vector Laboratories	B-1035	1000

*All antibodies were validated using positive and negative control tissue samples.

Table S4. Primers for RT-PCR			
Gene	**Forward Primer Sequence**	**Reverse Primer Sequence**	**Product Size**
ActB	CATAGCACAGCTTCTCTTTGATGTC	CTAAGGCCAACCGTGAAAAGATG	321 bp
PlexinA1	TCAATGACAAAGTTGCCATTCCAC	AAATACCGCCATGTTTGCACC	350 bp
PlexinA2	TGAGATGGTCTCTGTGTTCAAAGAT	GATCCCCTGAGCTTAGACACTCT	167 bp
PlexinA3	CTGTTGGATACTGTGTACAAGGGTA	GCTATCCGGGCTGCTGG	301 bp
PlexinA4	CACAATGGGGGTCACCTGAG	AAATGCCCTCCAATATGAGACTGT	188 bp
PlexinB1	ATGCTGGGGAGTATGATGTCTCTA	GAGCTTAGAACCATGCAGGGTAA	214 bp
PlexinB2	GCAGTCATAGAAGGGATACTGGTG	GACTGAGGACGATGAGTTACTGTG	206 bp
Nrp1	GGCCCTTTCTCTTCATCAAATTTGT	CTCCAGGTCAAAACTTTCAAACTCC	214 bp
Nrp2	TACATCAAGTTCACCTCAGACTACG	CAGCCAGTCATATTTACAGTCTCCT	254 bp